Arch. Mech., 41, 4, pp. 427–460, Warszawa 1989

An internal variable theory of inelastic behaviour at high rates of strain

O. T. BRUHNS and H. DIEHL (BOCHUM)

THE OBJECTIVE of the present paper is the formulation of the general frame of an internal variable theory of high strain rate deformations in metals. Such deformations are characterized by nucleation, growth and coalescence of various microdefects like shear bands, cracks and voids. Localized deformations in the vicinity of these microdefects as well as dislocation motion in the remaining parts of the body contribute to the inelastic strain rate. After identification of appropriate internal variables through an approximate homogenization procedure, evolution laws and flow rules are introduced and investigated with respect to their consistency with thermodynamics. The Clausius–Duhem inequality is utilized as a measure of irreversibility. Introducing a polynomial representation of specific free enthalpy, thermodynamically consistent evolution laws are derived. Finally, the theory is applied to the problem of propagation of uniaxial acceleration waves into an unstressed homogeneous medium.

Celem pracy jest sformułowanie ogólnych zasad teorii zmiennych wewnętrznych przy dużych prędkościach odkształcenia metali. Odkształcenia takie charakteryzują się nukleacją, wzrostem i koalescencją różnych defektów, takich jak pasma ścinania szczeliny i pustki. Zlokalizowane deformacje w otoczeniu tych mikro-defektów jak również ruch dyslokacji w pozostałych obszarach prowadzą do pojawienia się niesprężystych prędkości odkształcenia. Po identyfikacji stosowanych zmiennych wewnętrznych, drogą przybliżonej homogenizacji, wprowadzono prawa ewolucji i uplastycznienia badając je z punktu widzenia ich zgodności z termodynamiką. Za miarę nieodwracalności przyjęto nierówność Clausiusa–Duhema. Wprowadzenie wielomianowej reprezentacji swobodnej entalpii właściwej umożliwiło wywód zgodnych z termodynamiką praw ewolucji. Teorię zastosowano na koniec do problemu propagacji jednowymiarowych fal przyspieszenia w jednorodnym ośrodku beznaprężeniowym.

Целью работы является формулировка общих принципов теории внутренних переменных при больших скоростях деформации металлов. Такие деформации характеризуются нуклеацией, ростом и коалесценцией разных дефектов, таких как полосы сдвига, трещины и пустоты. Локализированные деформации в окрестности этих микродефектов, как тоже движение дислокаций в остальных областях, приводят к появлению неупругих скоростей дефформации. После идентификации соответствующих внутренних переменных, путем приближенной гомогенизации, введены законы эволюции и пластичности, исследуя их с точки зрения совместимости с термодинамикой. За меру необратимости принято неравенство Клаузиуса-Дюгема. Введение многочленного представления свободной удельной энтальпии дает возможность вывода совместимых с термодинамикой законов эволюции. Наконец, теория применена к задаче распространения одномерных волн ускорения в однородной безнапряженной среде.

General notation

- $\boldsymbol{\sigma}$ Cauchy stress tensor,
- $\boldsymbol{\epsilon}$ linearized Green's strain tensor,
- θ absolute temperature,
- g specific free enthalpy,
- $\mathbf{q}$ heat flux,
- $\mathbf{Z}^0$ damage tensor.

For arbitrary second order tensors $\mathbf{A}, \mathbf{B}$ we use

$\mathbf{AB} \Leftrightarrow A_{ij}B_{jk}$,

$\mathbf{A} \cdot \mathbf{B} \Leftrightarrow A_{ij}B_{ij}$,

$\mathrm{tr}\mathbf{A} \Leftrightarrow A_{ii}$,

Further notation is explained in the text.

1. Introduction

THE BEHAVIOUR of metals under dynamic loading (impact, explosive forming) has been explored for about half a century. The classical papers by TAYLOR [53] and v. KÁRMÁN and DUWEZ [19] on theoretical and experimental determination of the "dynamic yield stress" can be considered as the foundation stones of dynamic plasticity. For many years the theory of rigid-ideally-plastic bodies with a yield stress taken from dynamic tests was fundamental to the design of dynamically-loaded structures.

Several approximate theories, e.g., based on extremum principles, have been developed by MARTIN, SYMONDS, KALISZKY and others [18, 29, 52]. These theories provide reliable information as long as

a) the external energy input is several times greater than the total elastic strain energy capacity,

b) $|\varrho\dot{\mathbf{v}}| \gg |\mathrm{div}\boldsymbol{\sigma}'|$ holds,

c) the strain rate is approximately constant,

d) the characteristic external times are large compared with l/c, where l is a typical dimension of the structure and c is a typical velocity of wave propagation,

e) the process can be regarded as isothermal.

The violation of one of these presuppositions requires the use of more sophisticated constitutive models. Thus first corrections were concerned with the dependence on strain rate and temperature. We mention some simple extensions of the rigid plastic model where the originally constant yield stress is replaced by a function of $\dot{\boldsymbol{\epsilon}}$, θ and the more elaborated overstress models by PERZYNA and SOKOLOVSKI-MALVERN [36, 28].

These models, however, are of pure phenomenological character and therefore show some disadvantages:

The complex behaviour under high strain rate loading requires a large number of material functions and parameters, where only a few independent experiments are available.

Phenomenological models are intended for stress analysis and do not contain failure criteria.

These disadvantages have provoked the desire of incorporating micromechanics (deformation and damage mechanisms) into a continuum theory of high strain rate deformations. The micromechanics of high strain rate deformations, namely, have been studied extensively (see for instance the conference proceedings [15, 16, 20, 31, 34, 41]). Metallurgy traditionally concentrates on the behaviour of isolated lattice defects rather than on defect accumulation and the published results on isolated defects are only partially useful for the continuum physicist. It was not until the mid-seventies that the first systematic studies on high strain rate damage were published by the SRI group, to which we owe almost everything that is known about microdamage under dynamic loading [9, 10, 45, 48, 49, 50].

It was found that in addition to the motion of dislocations, three-dimensional lattice defects (pre-existing flaws, inclusions) determine the material's behaviour. An improved continuum theory of dislocation-induced deformations at high strain rates is due to PERZYNA [37, 38]. Continuum damage theories of dynamically-loaded bodies have been published by the SRI group [9] and by PERZYNA [40]. Perzyna investigated isothermal damage processes due to ductile microcracks in the context of an internal variable theory.

The objective of our paper is the development of a continuum damage theory of non-isothermal high strain rate processes with particular attention to shear band formation. Section 2 contains a review of experimental observations and their physical interpretations. Conclusions about the applicability of the classical continuum theory and the general frame of an internal variable theory are presented in Sects. 3 and 4. Section 5 deals with the identification of internal variables describing micro-shear bands. Criteria for the assessment of shear band damage are derived in Sect. 6. They describe the failure of material volume elements, not of engineering structures. Flow rules and evolution laws describing dislocation mechanisms at slow, moderate and high strain rates up to 10^4 s^{-1} are given in Sect. 7. The constitutive laws introduced so far will be inspected as to their consistency with the second law of thermodynamics in Sect. 8. The second law is expressed in terms of the Clausius–Duhem inequality with the free enthalpy function as the thermodynamic potential. The constitutive model is specialized to the case of uniaxial states of stress in Sect. 9. These equations are used to study some aspects of propagation of acceleration waves (propagation velocity, "transport equation" of the acceleration jump).

The main features of our model are summarized in Sect. 10 and necessary extensions left to future work are outlined.

2. Experimental observations and their physical interpretation

2.1. General considerations

I. Classification of experimental methods

Dynamic experiments can be divided into two categories:

a) Measurement of the time history of macroscopic observables ($\boldsymbol{\epsilon}$, $\dot{\boldsymbol{\epsilon}}$, $\boldsymbol{\sigma}$, θ) and construction of σ-ε-diagrams, σ-$\dot{\varepsilon}$-diagrams (see paragraph II).

b) Inspection of structural changes (dislocation density, void density...) after a high rate loading (see paragraph III).

Details about the experimental apparatus can be found in [15, 16, 31].

II. i. σ-ε and σ-$\dot{\varepsilon}$-curves are determined by either flat plate impact tests, expanding ring tests or several modifications of the split Hopkinson bar. Strain rates of some 10^4 s^{-1}

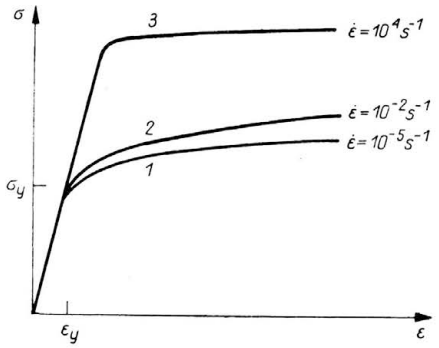

FIG. 1. Typical stress-strain relations for various constant strain rates.

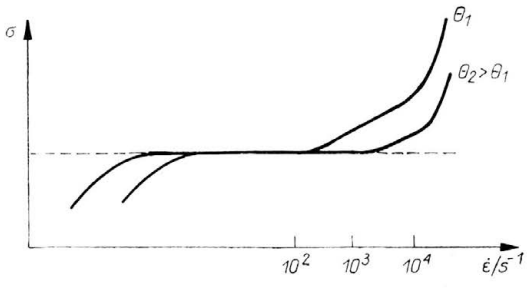

FIG. 2. Typical stress-strain rate relations for constant strain and various temperatures.

can be realized with polycrystalline specimens. However, equivalent strain rates in biaxial loading are restricted to no more than 200 s^{-1}. Typical σ-ε, σ-$\dot{\varepsilon}$-diagrams are depicted in Figs. 1 and 2.

From Fig. 1 we see that the phenomenological yield limit σ_y as well as the tangent modulus E_t depend on strain rate. $\partial\sigma_y/\partial\dot{\varepsilon} \neq 0$ is more or less pronounced depending on the composition and crystal structure. For $\dot{\varepsilon} < 1\ s^{-1}$ and $\theta = \text{const}$ E_t increases with

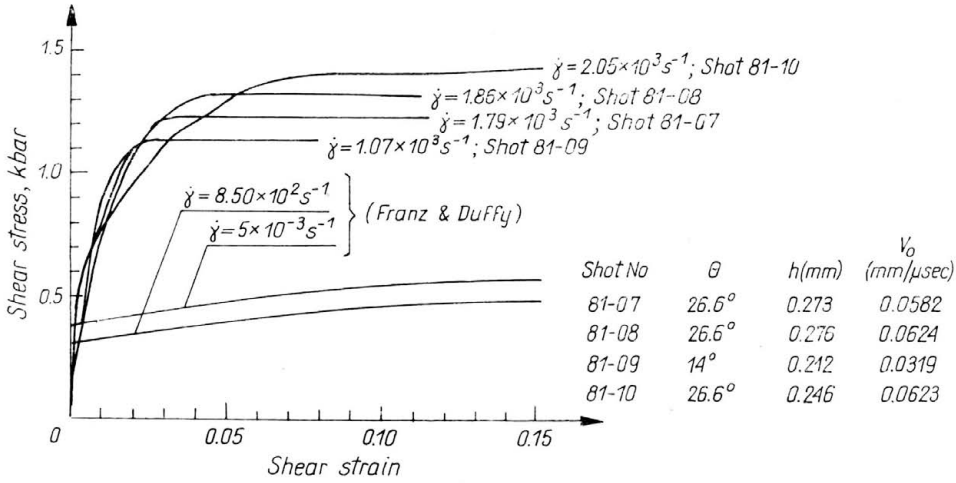

FIG. 3. Dynamic stress-strain curves for 1100-0 aluminium (from ref. [7]).

$\dot{\varepsilon}$ (curves *1*, *2*). At extremely high rates (curve *3*) adiabatic heating and damage result in a decrease of E_t whose amount is not known exactly. The curves drawn in Fig. 1 schematically are in some respect oversimplified, e.g., the difference between the isothermal and the adiabatic Young's modulus is neglected. Figures 3 and 4 show stress-strain-curves for aluminium and Nitronic 40.

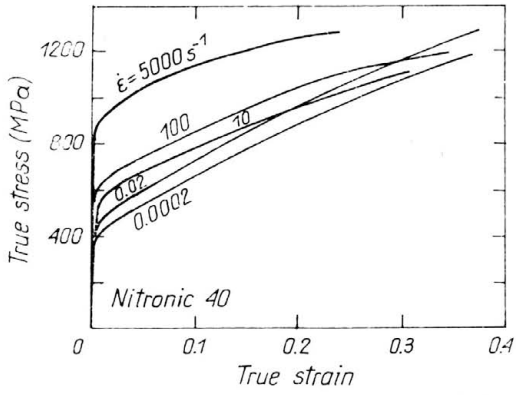

FIG. 4. Stress-strain curves for Nitronic 40 stainless steel (from ref. [12]).

ii. Stress-strain rate diagrams enable us to identify regions of different rate controlling deformation mechanisms [13, 37]. Usually ε is taken to be an offset strain (say 2%) and the curves are then called yield stress-strain rate curves. Figure 2 shows the significant increase

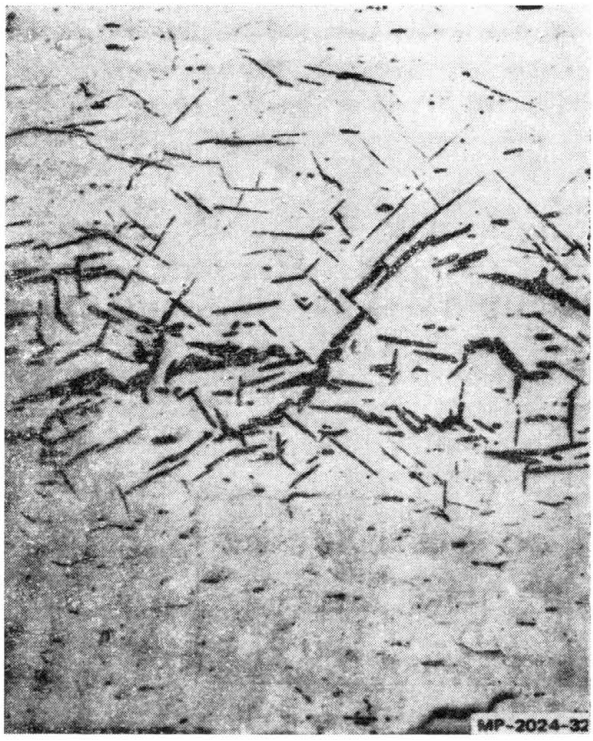

FIG. 5. Polished cross section in shock-loaded Armco iron revealing internal cleavage cracks (from ref. [48]).

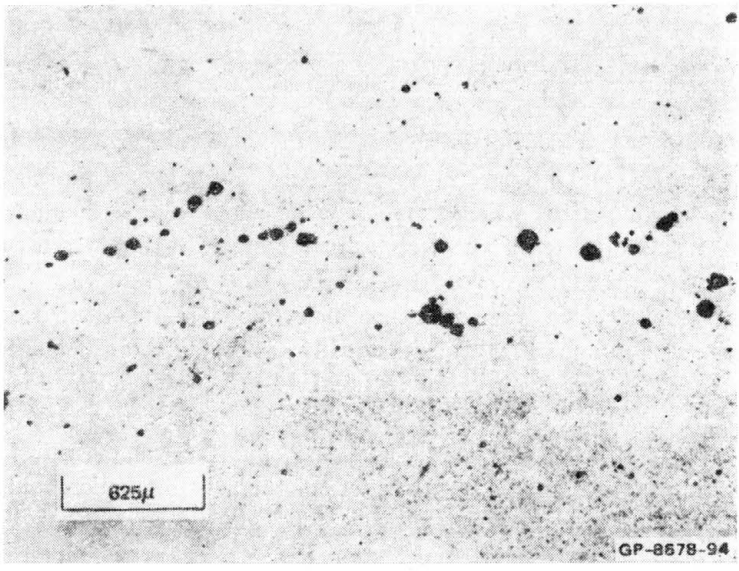

FIG. 6. Polished cross section in shock-loaded 1145 aluminium showing the population of internal spherical voids (from ref. [48]).

of strain rate sensitivity $\partial \ln \sigma / \partial \ln \dot{\varepsilon}$ at strain rates of the order 10^3 s^{-1}, ..., 10^4 s^{-1}. This increase will be discussed in Sect. 2.3.

III. i. Depending on material and loading conditions, high strain rate failure of solids occurs through nucleation, growth and coalescence of cracks, voids or shear bands [48]. Typical defect arrangements are shown in Figs. 5 to 7. The occurrence of voids and shear

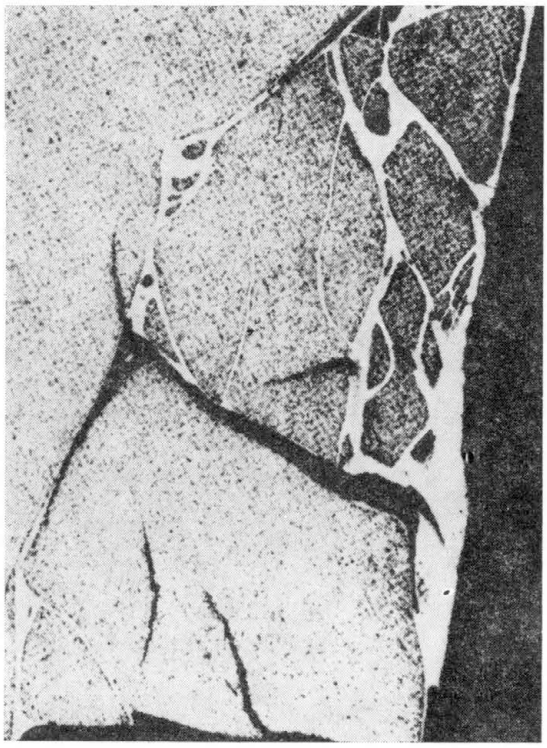

FIG. 7. Adiabatic shear zones near the plugged region in an ESR steel plate (from ref. [34]).

bands at small overall strains distinguishes damage at high rates from well-known ductile failure at low rates. It was observed that under short-lived tensile pulses, materials fail by either microcracking or by void formation while under high rate compressive pulses, shear bands are developed [48]. The tests were performed at strain rates up to 10^4 s^{-1} [45].

ii. It is generally assumed that any approach of modelling micro-structural high rate failure processes in a continuum theory is equally applicable to all damage modes. This hypothesis is based on the observation of "weak spots", where nucleation of defects is preferred [49, 10]. Possible weak spots are inclusions, pre-existing microcracks, grain junctions in inclusion-free grain boundaries [43]. While the role of inclusions and grain junctions is generally accepted in the case of microcracks and microvoids, the nature of the weak spots in shear-band processes is still controversial [49].

CURRAN *et al.* [10] describe void nucleation and growth by a general evolution law taking into account vacancy diffusion as well as mechanical debonding due to increasing mean stress and plastic strain. Plastic flow controlled growth was also assumed by PERZYNA

[40]. As to the use of plastic flow controlled laws, we quote from Curran et al.: "*We assume that nucleation at any heterogeneity requires a combination of local stresses normal and tangential to the heterogeneity... plastic shear strain is probably a better indicator of the local shear stress than is the continuum shear stress*". Thus the use of plastic strain is merely a substitute for a measure of local stress, which cannot be registered in the continuum theories of Curran et al. and Perzyna.

It is interesting to know whether defect generation at high rates is due to the damage mechanisms which are already known to be responsible for damage at slow rates. In the case of void formation, Curran et al. conclude: "*there is nothing unique about high rate loads; they simply explore particular areas of the microvoid kinetics*". A generalization of this statement to other defects can be questioned, especially in the case of shear bands.

iii. Local stress concentrations (phenomenologically described as weak spots) are removed by local dislocation motion at slow rates. With increasing strain rate more and more dislocations are "frozen in" and the local stresses may overcome a nucleation threshold. The importance of stress concentrators may be expected to cease with increasing overall stress. If the overall shear stress reaches values of the order $\mu/10$ (a value not uncommon in shock waves), homogeneous defect nucleation may occur (e.g. homogeneous nucleation of dislocations [32]).

IV. The irreversible deformations due to localized shear, slip or void opening, causing fragmentation on the microscale, superpose conventional dislocation induced deformations. Many experiments were performed to study dislocation density and spatial dislocation distribution after a high rate loading of single crystals and polycrystals [32, 6]. The main results are:

The dislocation density N at constant ε increases with $\dot{\varepsilon}$, i.e., the evolution of N proceeds rate dependent ([12], comparison of data from [6], [2]).

The spatial distribution of dislocations is much more homogeneous than at slow rates. There is little formation of dislocation arrangements, e.g., if cells are formed at all, they are smaller than the cells observed at slow rates [32].

The differences between local plastic strain at constant overall ε decrease with increasing strain rate because high stresses permit slip or even multiple slip in unfavourably oriented grains.

Twin formation is favoured, especially in materials with low stacking fault energy.

A further discussion of dislocation mechanics at high rates follows in Sect. 2.3.

2.2. Shear band observations and their interpretation

I. Shear bands are surfaces with a reduced capacity for carrying shear-stresses and are deposited in a dynamically-loaded solid body with a density of $10^3/\text{cm}^3$ to $10^5/\text{cm}^3$. Their geometry resembles that of edge dislocations. In many materials, shear bands produced during high loading rates form not etchable, white bands. The white bands suggest the occurrence of a localized increase of temperature causing a phase transformation. Shear band dimensions vary over a wide range from some microns up to a few mm; larger bands occur due to coalescence in the final process of fragmentation.

Typically shear band dimensions are larger than the grain diameter d and the spreading of shear bands is not influenced by grain boundaries (see Fig. 8). Unfortunately, the publications of the SRI do not provide a systematic study of shear band orientations. If we assume that during the CFC-test [49] plain stress and radial loading prevail, we can

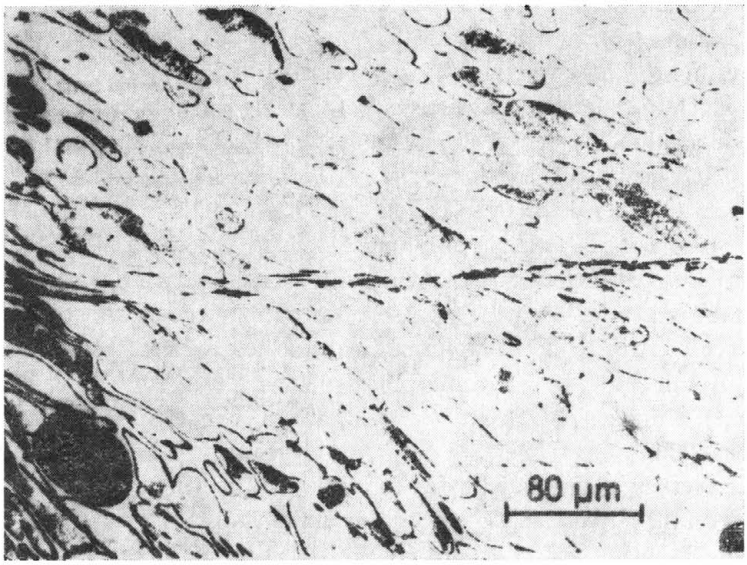

FIG. 8. Propagation of an adiabatic shear band in a tungsten sinter alloy (from ref. [42]).

conclude that under such conditions most of the shear bands are aligned with the principle stress trajectories.

II. Currently, different types of shear localizations are known. A survey of shear localizations at small strain rates and large strains is presented by ASARO [2]. Shear band phenomena are classified according to their geometrical extensions. We distinguish

localized shear zones in individual crystallites (kink bands, coarse slip bands, "macroscopic" shear bands),

localized shear zones spreading over several grains (deformation shear bands).

Shear bands in dynamically loaded materials belong to the second category. None of the shear localizations mentioned above is accompanied by high temperatures or phase transformations. Texture softening after large strains has been suggested as a nucleation mechanism. There seem to be typical shear band nucleation mechanisms at high strain rates, namely adiabatic shear [13] or catastrophic "Frenkel's" shear. By catastrophic shear we mean the athermal slip of crystallographic planes without the aid of dislocations. This mechanism was erroneously suggested by Frenkel as the reason of ductility at slow rates before the discovery of dislocations.

2.3. Further remarks on the contribution of dislocation mechanisms

I. Discussion of the increase of strain rate sensitivity at $\dot{\varepsilon} \approx 10^4\ s^{-1}$

i. In the following we examine a polycrystalline volume element ΔV and a single crystal volume element δV cut from ΔV. In the case of quasi-stationary dislocation glide, the

average dislocation-induced strain rate $\dot{\gamma}_d$ of δV can be expressed through Orowan's equation as follows [25]:

$$\dot{\gamma}_d = \operatorname{sym}\Big(\sum_\alpha \dot{a}_\alpha \mathbf{m}_\alpha \otimes \mathbf{n}_\alpha\Big), \tag{2.1}$$

$$\dot{a}_\alpha = \frac{b_\alpha^2 N_m^\alpha}{\exp\left(\dfrac{\Delta g}{k\theta}\right)\left(2\nu_D \sinh \dfrac{\tau_\alpha^* b_\alpha l \Delta x}{k\theta}\right)^{-1} + \dfrac{B}{\tau_\alpha^*}}, \tag{2.2}$$

where the sum extends over all active glide systems in δV with normal $\mathbf{n}_\alpha$, glide directions $\mathbf{m}_\alpha$ and Burgers vector b_α. The shear rate $\dot{a}_\alpha$ is determined by the mobile dislocation density N_m^α, the effective shear stress $\tau_\alpha^* = \tau_\alpha - \tau_{\mu\alpha}$, i.e., the difference between resolved shear stress and athermal stress, the free enthalpy Δg which must be supplied to push a dislocation over a weak obstacle in the case of $\tau_\alpha^* = 0$, the activation volume $b_\alpha l \Delta x$, the Debye frequency ν_D, Boltzmann's constant k and a so-called drag coefficient B. The first term in the denominator represents thermally-activated glide, the second term drag-controlled glide. Several special cases can be extracted from Eq. (2.2): very large τ_α^*, dislocations may overcome the barrier Δg without thermal activation and the resulting shear rate is controlled by the dependence of the flight velocity on several interactions like phonon scattering, electron scattering and the like. These effects are summarized in the drag constant B. Small values of τ_α^* result in thermally-activated glide and at even lower effective shear stresses $\tau_\alpha^* \approx 0$ Eq. (2.2) may be replaced by a rate-independent flow rule describing athermal glide motion (see [25]).

The increased strain-rate sensitivity at strain rates of the order of 10^4 s^{-1} has repeatedly been attributed to drag effects [26, 37, 47]. Very recently objections have been raised against this interpretation [12]:

The change in strain rate sensitivity can also be explained by a rate-dependent increase of total dislocation density.

ii. Four reasons prohibit the application of Orowan's equation to high strain rate processes:

a) Later on we will be interested in the average dislocation-induced deformation $\dot{\boldsymbol{\epsilon}}_d$ of ΔV which results from all the δV contained in ΔV. Due to the fluctuations of the resolved shear stress, $\dot{\boldsymbol{\epsilon}}_d$ contains contributions from grains with different activated deformation mechanisms. The total dislocation induced deformation simultaneously exhibits athermal, thermally-activated or drag-controlled dislocation motion.

b) Cross-slip and climb are neglected in Eq. (2.1). However, cross slip may be important during a high-rate loading and climb may be initiated during recovery under high temperatures following a high-strain-rate deformation.

c) Eq. (2.1) does not take into account deformations due to twinning.

d) As was already mentioned, the Orowan equation is restricted to quasi-stationary flight motion. MECKING [30] and PERZYNA and PECHERSKI [39] discussed generalizations which, for single slip, are given by

$$\dot{\gamma}_d = \dot{a} + b d \dot{N}_m. \tag{2.3}$$

$\dot{N}_m$ is the rate of production of mobile dislocations. It is believed that $\dot{N}_m$ is controlled by athermal mechanisms [39]. In addition to athermal glide in grains with small τ^*, this is another source of athermal behaviour.

II. While total dislocation density can be measured quite accurately for $N < 10^{14}$ m^{-2}, there is some uncertainty about the values of mobile dislocation density at high strain rates. Extrapolation of formulae derived for small rates gives unrealistically large values of N_m. Direct measurement of N_m was performed by SHIOIRI [46, 47] at strain rates up to $8 \cdot 10^3$ s^{-1}. A slow increase of N_m with $\dot{\varepsilon}$ was observed, which was below the increase of total dislocation density with $\dot{\varepsilon}$. We conclude that the ratio N_m/N decreases with increasing strain rate.

Very few evolution laws for N_m can be found in the literature. In most cases N_m/N is assumed to be a constant of the order of 10^{-2}. A rate-independent evolution law $\dot{N}_m = (N_m/N + Nf(N))\,\dot{N}$ was suggested by GILMAN (see [21]).

III. Widely different suggestions for evolution laws of N can be found in the literature. A comparison of these suggestions is beyond the scope of this article. The equations intended to be valid for small and moderate strain rates typically have the form

$$\dot{N} = k_1(\cdot)\dot{\gamma}_d - k_2(\cdot). \tag{2.4}$$

Dislocation generation is governed by plastic flow while $-k_2$ corresponds to annihilation. Restriction to small strain analysis allows for the neglect of $-k_2$. Often $k_1 = \text{const}$ is assumed for slow processes. ZSLODOS and KOVACS [54] suggest $k_1 = \alpha\tau$, $\alpha = \text{const}$. This corresponds to the use of plastic work as a measure of hardening in phenomenological theories of plasticity.

In order to describe rate-dependent dislocation generation at high strain rates, KLEPACZKO [22] suggested a nonlinear dependence on $\dot{\gamma}_d$:

$$\dot{N} = k_1(\dot{\gamma}_d)\dot{\gamma}_d. \tag{2.5}$$

GILMAN [14] introduced an evolution law of the type

$$\dot{N} = k_1(\cdot)\dot{\gamma}_d + \hat{N}\exp(-\mu/\sigma), \tag{2.6}$$

where the second term describes homogeneous nucleation of dislocations at large σ/μ, i.e., at high strain rates.

A drastic increase of dislocation density has been observed in shock-loaded materials. Since it is believed that dislocations are generated at the wave-front and are rearranged behind the wave-front [32], one might ask for a jump condition giving the jump $[N]$ in terms of $[\boldsymbol{\sigma}]$, $[\mathbf{v}]$, $[\theta]$. None of the equations mentioned above allows for the calculation of $[N]$. STOUT [51] developed a generalized dislocation theory with a balance law for N of the Boltzmann-type and derived $[N]$.

IV. Remark on latent energy in high strain-rate processes:

It is known that only 90–95% of plastic work is converted into heat, the rest is stored as an internal stress energy. The latent energy of a polycrystal is determined by two types of internal stresses, namely internal stresses fluctuating with the mean separation distance of single dislocations and with the grain diameter, respectively. The contribution of the former probably increases with strain-rate because of the lack of time for dislocation

arrangement. However, the stress variations between adjacent grains are less pronounced at high rates.

Nothing can be said about the fraction of latent energy. Since stress variations between adjacent grains are responsible for the Bauschinger effect, we might expect that anisotropic hardening is less pronounced at high strain rates.

3. Conclusions about the applicability of a local continuum theory

I. Let $P \in B$ be a material point of a body B with current location $\mathbf{x} \in \chi_t$. P is defined by attaching average quantities taken over a representative volume element ΔV whose dimensions are chosen such that

$$l_s \ll \sqrt[3]{\Delta V} \ll l_e, \tag{3.1}$$

where l_s is a characteristic length of the material's substructure (e.g., the diameter of or the distance between shear bands) and l_e is a characteristic length of the applied load. In wave propagation problems l_e can be chosen as $v_0 c_0/|[\dot{v}]|$, where c_0 is the largest velocity of acceleration waves, v_0 is an impact velocity and $[\dot{v}]$ is the jump of the acceleration across the wave-front. Thus the right inequality in Eq. (3.1) expresses an upper bound $v_{\max}$ of v_0. If $v_0 > v_{\max}$, an inadmissible increase of v results and ΔV is no longer typical and probably a nonlocal theory is appropriate. In the present case ΔV is a polycrystal containing a finite number of defects with the diameter $< \sqrt[3]{\Delta V}$ (henceforth called micro-defects). Sometimes it will be useful to study the volume element δV cut from a single crystal as well. The relationship between χ_t, ΔV and δV is sketched in Fig. 9. Following

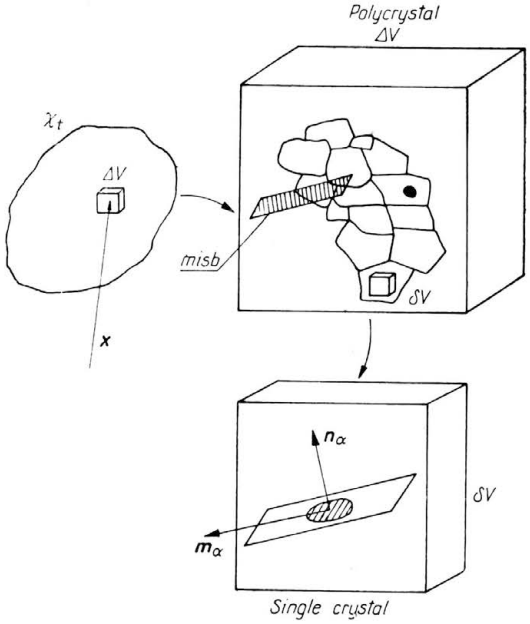

FIG. 9. Illustration of the relation between the volume elements ΔV and δV.

[5] we take $[\dot{v}] = v_0/t_r$ with the rise time t_r and write $\sqrt[3]{\Delta V}$ as a multiple of the grain diameter d. Therefore the inequality (3.1) can be written as

$$l_s \ll nd \ll c_0 t_r, \quad t_r = v_0/|[\dot{v}]|. \tag{3.2}$$

For typical values of c_0, t_r, d, n is of the order 10 to 100.

II. The basic postulate of continuum mechanics is that the motion $\mathbf{x}(\mathbf{X}, t)$ is a continuous function of $\mathbf{X}$, i.e., adjacent volume elements remain adjacent during the whole process. This condition is violated by growth and coalescence of defects. Only defects with dimensions $< \sqrt[3]{\Delta V}$ can be described in the framework of the classical continuum theory and may be considered "smeared out" over the actual configuration χ_t. Larger defects ("macrodefects") grow in the course of the process and must be treated as individual perturbations of the body's topology. Necessarily the calculation of a high strain rate deformation proceeds in two periods:

P1 $0 \leqslant t \leqslant t^*(\mathbf{x})$,

P2 $t > t^*(\mathbf{x})$,

where $t^*(\mathbf{x})$ is the time at which a macrodefect is nucleated in $\mathbf{x}$.

III. The objective of our paper is a description of P1. A small strain formulation is sufficient in many applications (e.g., plugging, spalling) and will be employed. As mentioned in Sect. 2, there are well-defined regimes where shear banding is the dominant damage mechanism and the restriction of a general damage theory to a theory of micro-shear bands (henceforth abbreviated as misbs) makes sense. As long as the misbs can be considered "smeared out", there is no need to determine size distributions. In this respect our theory differs from the formulations of CURRAN [9] and PERZYNA [40].

A necessary condition for an extension of the model to P2 (e.g., via FE-calculations with mesh-reorganization at macrodefects) is that the time of nucleation as well as the size and orientation of a macrodefect are determined by the continuum damage theory.

Throughout the paper we assume that homogeneous nucleation of defects is prevented by a restriction to such processes where nucleation at weak spots is verified experimentally, i.e., for strain rates up to 10^4 s^{-1}. We have repeatedly pointed out the importance of stress concentrations and/or local hot spots for nucleation and growth of microdefects and continuum measures of stress concentrations and hot spots are highly desirable.

4. Genaral frame of a continuum theory with internal and process variables

I. The concept of internal and process variables has been discussed extensively in the literature. We briefly summarize the ideas.

i. In addition to macroscopic variables ($\boldsymbol{\sigma}, \theta, \boldsymbol{\epsilon}, \mathbf{q}, g, e$), further quantities are introduced to describe the internal mechanical state of an inelastically deformed polycrystalline material. Devices on a microscopic scale are necessary to make these quantities visible. Such a quantity is called an internal variable p if changes of p result in a change of internal energy (e.g., total dislocation density, void density). Other quantities $\bar{p}$ of interest which do not alter the internal energy are called process variables (e.g., mobile dislocation density, preferred directions).

ii. In the present case we introduce two sets of internal and process variables, respectively:

$\{S_i\}$ set of internal variables describing shear band processes,
$\{D_i\}$ set of internal variables describing dislocation processes,
$\{\bar{S}_i\}$ set of process variables describing shear band processes,
$\{\bar{D}_i\}$ set of process variables describing dislocation processes.

II. Total strain is decomposed into reversible and irreversible parts according to

$$\boldsymbol{\epsilon} = \boldsymbol{\epsilon}_r + \boldsymbol{\epsilon}_i . \tag{4.1}$$

$\boldsymbol{\epsilon}_i$ is further decomposed into dislocation-induced strains and strains due to accumulated localized shearing and slip along misbs:

$$\boldsymbol{\epsilon}_i = \boldsymbol{\epsilon}_d + \boldsymbol{\epsilon}_s . \tag{4.2}$$

$\boldsymbol{\epsilon}_d$ represents contributions of different dislocation mechanisms. From the discussion of Sect. 2, it follows that

$$\boldsymbol{\epsilon}_d = \boldsymbol{\epsilon}_{da} + \boldsymbol{\epsilon}_{dt} + \boldsymbol{\epsilon}_{dd} . \tag{4.3}$$

Here $\boldsymbol{\epsilon}_{da}$ is the average effect of athermal dislocation motion in the disproportionately stressed grains of ΔV and similar interpretations are given to $\boldsymbol{\epsilon}_{dt}$, $\boldsymbol{\epsilon}_{dd}$ in connection with thermally activated dislocation motion and drag-controlled dislocation motion, respectively. In general, one of the three terms in Eq. (4.3) will dominate, e.g., $\|\boldsymbol{\epsilon}_{da}\| \gg \|\boldsymbol{\epsilon}_{dt}\|$, $\|\boldsymbol{\epsilon}_{dd}\|$ at low temperatures and strain rates. However, the decomposition (4.3) is fundamental for a continuous behaviour over a wide range of strain rates. The different contributions of $\boldsymbol{\epsilon}_i$ are subjected to different yield and loading conditions. In some respect $\dot{\varepsilon} = 10^4\ \mathrm{s}^{-1}$ has the meaning of a limiting strain rate. It characterizes the beginning of a significant contribution of drag mechanisms, it is the current upper limit of the regime of discrete defect generation at weak spots and it is related to the maximum admissible velocity v_0 in Eq. (3.2). In what follows we shall restrict our considerations to strain rates less than $10^4\ \mathrm{s}^{-1}$ and will thus neglect $\boldsymbol{\epsilon}_{dd}$ in Eq. (4.3).

III. The constitutive law for a material undergoing inelastic deformations well into the regime of high strain rates up to $10^4\ \mathrm{s}^{-1}$ comprehends

a) one function $\bar{g}(\boldsymbol{\sigma}, \theta, S_i, D_i)$ specifying the free enthalpy,
b) flow rules for $\dot{\boldsymbol{\epsilon}}_s$, $\dot{\boldsymbol{\epsilon}}_{da}$, $\dot{\boldsymbol{\epsilon}}_{dt}$ and associated yield and loading conditions,
c) evolution laws for S_i, D_i, $\bar{S}_i$, $\bar{D}_i$,
d) the law of heat flux.

In the following Section we shall identify the internal and process variables and postulate general representations of the corresponding growth laws. These equations are subjected to the second law of thermodynamics in Sect. 8.

IV. In constructing general representations of the evolution laws, the following principles are formulated and will be observed:

PRINCIPLE 1. The complete set of balance laws and constitutive laws constitutes a quasi-linear hyperbolic system.

PRINCIPLE 2. The left-hand side of the Clausius–Duhem inequality is piecewise linear in the rates of the macroscopic variables.

PRINCIPLE 3. (Decoupling of dislocation and shear band processes at the macroscale): The evolution of the S_i, $\bar{S}_i$ is independent of the D_i, $\bar{D}_i$ and *vice versa*.

Of course, there is a coupling between different deformation mechanisms on the microscale which will be taken into account by the definition of the $\bar{S}_i$.

Principle 1 has an obvious physical interpretation. Principle 2 is more or less a matter of convenience to comply with the usual methods of evaluating the Clausius–Duhem-inequality. Both principles rule out oversimplified descriptions of rate-dependent behaviour like Eq. (2.5) for the dislocation density or PERZYNA's [39] concept of an $\dot{\boldsymbol{\epsilon}}$-dependent control function in the flow rule for $\dot{\boldsymbol{\epsilon}}_d$.

Further principles will be introduced later on.

IV. i. To simplify the notation, a few abbreviations of the general form of evolution laws to be considered in Sects. 5 and 7 will be given here. Let $\mathbf{Y}$ be a representative element of $\{D_i\}\cup\{\bar{D}_i\}$, say. (The case $\mathbf{Y}\in\{S_i\}\cup\{\bar{S}_i\}$ can be dealt with analogously). Changes in $\mathbf{Y}$ may be due to either athermal or thermally activated mechanisms and may therefore be idealized as either rate-independent and instantaneous or rate-dependent and delayed:

$$\dot{\mathbf{Y}} = \dot{\mathbf{Y}}_{\text{inst}} + \dot{\mathbf{Y}}^*, \tag{4.4}$$

$$\dot{\mathbf{Y}}_{\text{inst}} = \mathbf{f}_1(\boldsymbol{\sigma}, \theta, D_j, \bar{D}_j, \dot{\boldsymbol{\sigma}}, \dot{\theta}), \quad \mathbf{f}_1 \text{ hom. of degree 1 in } \dot{\boldsymbol{\sigma}}, \dot{\theta}, \tag{4.5}$$

$$\dot{\mathbf{Y}}^* = \mathbf{f}_2(\boldsymbol{\sigma}, \theta, D_j, \bar{D}_j), \tag{4.6}$$

where a star denotes dependence of a variable on present values. Let $F(\boldsymbol{\sigma}, \theta, D_i, \bar{D}_i)$ be a yield function such that $F \geqslant 0$ is necessary for $\dot{\mathbf{Y}} \neq \mathbf{0}$. The associated loading index is

$$LC := \frac{\partial F}{\partial \boldsymbol{\sigma}} \cdot \dot{\boldsymbol{\sigma}} + \frac{\partial F}{\partial \theta}\dot{\theta}. \tag{4.7}$$

We postulate continuity of $\dot{\mathbf{Y}}$ for continuous $\dot{\boldsymbol{\sigma}}$, $\dot{\theta}$, especially at changes from loading to unloading and *vice versa*. The evolution law for $\dot{\mathbf{Y}}_{\text{inst}}$ thus reads

$$\dot{\mathbf{Y}}_{\text{inst}} = \begin{cases} LC\,\mathbf{h}(\boldsymbol{\sigma}, \theta, D_j, \bar{D}_j) & \text{if} \quad LC > 0, \quad F \geqslant 0, \\ \mathbf{0} & \text{otherwise}, \end{cases} \tag{4.8}$$

and $\mathbf{h}$ has the additional property $\mathbf{h} \to \mathbf{0}$ for $F \to 0$. Equation (4.8) can be written in compact form with the aid of Maccauly-brackets

$$\langle LC\rangle = \begin{cases} \langle LC\rangle & \text{if} \quad LC > 0, \\ 0 & \text{otherwise}, \end{cases}$$

$$\{\mathbf{h}\} = \begin{cases} \mathbf{h} & \text{if} \quad F \geqslant 0, \\ \mathbf{0} & \text{otherwise}, \quad \mathbf{h} \to \mathbf{0} \quad \text{for} \quad F \to 0. \end{cases}$$

If both parts of $\dot{\mathbf{Y}}$ are subjected to the same yield condition, Eq. (4.4) can be written as

$$\dot{\mathbf{Y}} = \{d_y\}\langle LC\rangle \mathbf{n}_y + \{\dot{\mathbf{Y}}^*\}, \tag{4.9}$$

with $\mathbf{h} = d_y \mathbf{n}_y$ where $\mathbf{n}_y$ (not necessarily a unit tensor) gives the direction of instantaneous changes of $\mathbf{Y}$.

ii. In formulating constitutive laws which are claimed to be valid over a wide range of strain rates, the following problem frequently occurs:

The idealization of instantaneous changes of the internal mechanical state loses its validity with the decrease of the characteristic external time, i.e., with increasing strain rate.

One expects $||\dot{\mathbf{Y}}^*|| \gg ||\dot{\mathbf{Y}}_{\text{inst}}||$ at high rates at least for some of the internal variables. This is clearly impossible if d_y and $\dot{\mathbf{Y}}^*$ depend only on instantaneous values of rate-independent variables. Taking d_y, $\dot{\mathbf{Y}}^*$ as functions of $\dot{\boldsymbol{\epsilon}}$, $\dot{\theta}$ results in a violation of principles 1 and 2. Thus the following question arises:

Can one find a variable (internal or process) denoted by u, whose present value characterizes $\dot{\boldsymbol{\epsilon}}, \dot{\theta}$ in the following sense:

a) If $\dot{\boldsymbol{\epsilon}} \equiv \dot{\mathbf{e}} = \text{const}, \dot{\theta} \equiv \dot{\vartheta} = \text{const}$, then there exists a unique relation $u_\infty = u_\infty(\dot{\mathbf{e}}, \dot{\vartheta})$.

b) If arbitrary processes $\dot{\boldsymbol{\epsilon}}(t)$, $\dot{\theta}(t)$ are approximated by piecewise constant strain and temperature rates $\dot{\boldsymbol{\epsilon}} = \dot{\mathbf{e}}_i$, $\dot{\theta} = \dot{\vartheta}_i$ for $t_i < t < t_i + \Delta t_i = t_{i+1}$, and if $u_{\infty i} = u_\infty(\dot{\mathbf{e}}_i, \dot{\vartheta}_i)$ then the relaxation time of u must be small compared with Δt_i.

Indeed the considerations of Sect. 2.3 suggest that

$$u := \frac{N_m}{N} \tag{4.10}$$

is an appropriate measure of strain rate and $d_y = d_y(u, \ldots)$, $\dot{\mathbf{Y}} = \dot{\mathbf{Y}}^*(u, \ldots)$ enables us to describe the dominance of thermally-activated mechanisms at moderate and high strain rates. The questions a), b) are a challenge to the stability theory of ordinary differential equations. The answers will be discussed briefly in Sect. 7.

5. Constitutive modelling of micro-shear band processes

5.1. Internal and process variables

I. Consider the representative volume element ΔV depicted in Fig. 10. It contains a finite number N of stress concentrators C_α located at $\mathbf{y}_\alpha$, $\alpha \in I = \{1, \ldots, N\}$. Misbs are assumed to be nucleated at C_α and are modelled as planes $\delta\mathbf{A}_\alpha = \delta A_\alpha \mathbf{e}_\alpha$, $\alpha \in I_{SB} \subset I$, where I_{SB} is the subset of all C_α where misbs exist at time t. The substructure of the material is

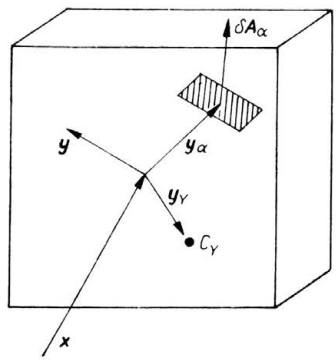

FIG. 10. A representative volume element ΔV of the damaged body with stress concentrators C_γ and micro-shear bands $\delta\mathbf{A}_\alpha$.

disturbed by the presence of these microdefects. We shall now introduce so-called "microfields" defined on ΔV, labelled by an index m and containing information about the behaviour at C_α. The nan approximate homogenization, particularly well-suited to the problem of a strongly disordered substructure, is employed to obtain continuum macrovariables.

Is should be noted that modelling stress concentrators as points C_α is already a heuristic approximation of the real volume element, where inclusions, microcracks etc. are finite regions $\delta V_\alpha \subset \Delta V$. To the best of the authors' knowledge there exists no method of calculation of the exact microfields in a volume element with arbitrary arranged δV_α embedded in an inelastic matrix. Therefore the approximate microfields (5.1), (5.2) are introduced *a priori*. It is hoped that they describe the essential features of the exact microfields.

II. Microfields are defined in the following way:

(5.1) i)
$$\boldsymbol{\sigma}_m(\mathbf{x}, \mathbf{y}, t) = \boldsymbol{\sigma}_{m1}(\mathbf{x}, \mathbf{y}, t) + \sum_{\alpha \in I} \Delta\boldsymbol{\sigma}_\alpha(t) \Delta V \delta(\mathbf{y} - \mathbf{y}_\alpha),$$

(5.2)
$$\theta_m(\mathbf{x}, \mathbf{y}, t) = \theta_{m1}(\mathbf{x}, \mathbf{y}, t) + \sum_{\alpha \in I} \Delta\theta_\alpha(t) \Delta V \delta(\mathbf{y} - \mathbf{y}_\alpha),$$

and similarly for $\boldsymbol{\epsilon}_d$, D_i, $\bar{D}_i$.

The first terms in Eq. (5.1) and (5.2) are called quasi-homogeneous parts since they describe the material in the absence of stress- and temperature concentrators. The latter are modelled by attaching additional stresses and temperatures to the C_α via Dirac's delta-distribution.

ii. We shall now define microfields characterizing the shear band processes. Obviously they have no quasi-homogeneous parts.

(5.3)
$$\mathbf{Z}_m(\mathbf{x}, \mathbf{y}, t) := \sum_{\alpha \in I_{SB}(t)} \delta A_\alpha(t) \Delta V \mathbf{e}_\alpha \otimes \mathbf{e}_\alpha \delta(\mathbf{y} - \mathbf{y}_\alpha)$$

is called the micro damage tensor and

(5.4)
$$\dot{\boldsymbol{\epsilon}}_{sm}(\mathbf{x}, \mathbf{y}, t) := \operatorname{sym}\Big(\sum_{\alpha \in I_{SB}(t)} (\dot{a}_\alpha \boldsymbol{\nu}_\alpha \otimes \mathbf{e}_\alpha \Delta V \delta_{A\alpha}(\mathbf{y} - \mathbf{y}_\alpha)\Big)$$

is the micro strain rate due to localized shearing and slip. $\delta_{A\alpha}$ is the delta-distribution associated with the plane $\delta\mathbf{A}_\alpha$ (see [33]). A further interpretation of $\mathbf{Z}_m$ will be given in Sect. 6 along with the discussion of failure criteria.

III. Homogenization of microfields

i. Let H_m be an arbitrary microfield, $H = \langle H_m \rangle$ denotes its average (in the present context the symbol $\langle\ \rangle$ shouldn't be confused with a Maccauly bracket) defined by

(5.5)
$$H(\mathbf{x}, t) = \langle H_m(\mathbf{x}, \mathbf{y}, t) \rangle := \frac{1}{\Delta V} \int_{\Delta V} H_m(\mathbf{x} + \mathbf{y}, t) f(\mathbf{y}) dV_y.$$

$f \in C^\infty(\Delta V)$ with $f(\xi) = f(|\xi|)$, $df/d|\xi| < 0$ is a weighting function. There are several reasons for the use of a weighted average instead of the average with $f \equiv 1$ usually employed in the theory of heterogeneous media. First of all, the use of $f \in C^\infty$ allows H_m to be a distribution. Secondly, classical homogenization procedures require either a periodic structure or a homogeneous deformation of $\partial\Delta V$ [24]. Neither of the two alternative requirements

is fulfilled in the presence of misbs. Thirdly, $f \in C^\infty$ enables us to write the result of Eq. (5.5) as a series of moments of H_m, which can be truncated after the desired degree of accuracy. Finally, the influence of $\partial \Delta V$ can be diminished by choosing a rapidly decreasing function f. In general, f needs not be specified. The averaging procedure (5.5) is well known in continuum electrodynamics [17] as the multipole expansion of Maxwell's laws.

ii. Inserting the microfields (5.1)–(5.4) into Eq. (5.5) leads to the following representation of the accompanying macrofields:

$$\begin{aligned} \boldsymbol{\sigma} &= \langle \boldsymbol{\sigma}_{m1} \rangle + \boldsymbol{\sigma}^0 - \operatorname{div} \boldsymbol{\sigma}^1 \pm \ldots, \\ \mathbf{Z} &= \mathbf{Z}^0 - \operatorname{div} \mathbf{Z}^1 \pm \ldots, \end{aligned} \tag{5.6}$$

$\mathbf{Z}$ is the macro-damage tensor (or damage tensor), expressed in terms of the moments $\mathbf{Z}^j$ of j-th order. For example,

$$\mathbf{Z}^0 = \Big\langle \sum_\alpha \delta A_\alpha \mathbf{e}_\alpha \otimes \mathbf{e}_\alpha \Delta V \delta(\mathbf{x}) \Big\rangle, \tag{5.7}$$

$$\mathbf{Z}^1 = \Big\langle \sum_\alpha \delta A_\alpha \mathbf{e}_\alpha \otimes \mathbf{e}_\alpha \otimes \mathbf{y}_\alpha \Delta V \delta(\mathbf{x}) \Big\rangle. \tag{5.8}$$

The average stress concentration $\boldsymbol{\sigma}^0 = \langle \Sigma \Delta \boldsymbol{\sigma}_\alpha \Delta V \delta(\mathbf{x}) \rangle$ will be called the stress concentration tensor. We will speak of a continuum theory of j-th order if the expansions (5.6) are truncated behind the moments of j-th order.

iii. The following estimations suggest that the simplest case of a zeroth-order continuum theory will already provide useful information. From the definition of the norm of higher order tensors

$$O(||\operatorname{div} \mathbf{Z}^{j+1}||/||\mathbf{Z}^j||) = \sqrt[3]{\Delta V}/l_e \ll 1 \quad \text{by assumption.} \tag{5.9}$$

In what follows we will restrict ourselves to the case of a zeroth-order theory where, for example,

$$\boldsymbol{\sigma} = \langle \boldsymbol{\sigma}_{m1} \rangle + \boldsymbol{\sigma}^0, \quad \theta = \langle \theta_{m1} \rangle + \theta^0. \tag{5.10}$$

The expressions in (5.10) may still be simplified since

$$||\langle \boldsymbol{\sigma}_{m1} \rangle|| \gg ||\boldsymbol{\sigma}^0|| \quad \text{though} \quad ||\boldsymbol{\sigma}_{m1}|| \ll ||\Delta \boldsymbol{\sigma}_\alpha||. \tag{5.11}$$

The relation (5.11) follows from the fact that the stress concentrations are restricted to a small neighbourhood of C_α. This is an analogy to the role of the dislocation core in dislocation mechanics. We conclude from the relation (5.11) and similar considerations that the zeroth moments may be neglected in comparison with the average of the quasi-homogeneous parts

$$\boldsymbol{\sigma} \approx \langle \boldsymbol{\sigma}_{m1} \rangle, \quad \theta \approx \langle \theta_{m1} \rangle, \quad \boldsymbol{\epsilon}_d \approx \langle \boldsymbol{\epsilon}_{dm1} \rangle, \ldots. \tag{5.12}$$

This simplifies the description of dislocation-induced processes.

iv. According to what has been said above, the continuum damage theory of zeroth order comprises the zeroth moments $\boldsymbol{\sigma}^0$, θ^0, $\boldsymbol{\epsilon}_d^0$, $\boldsymbol{\epsilon}_s^0$, $\mathbf{Z}^0$, D_i^0, $\bar{D}_i^0$. $\boldsymbol{\epsilon}_d^0$, D_i^0, $\bar{D}_i^0$ represent localized dislocation processes in the vicinity of stress concentrators. The interdependence of $\boldsymbol{\sigma}^0$, θ^0, $\boldsymbol{\epsilon}_d^0$, $\mathbf{Z}^0$ etc. expresses the interaction of different mechanisms on the microscale. If we assume that local hardening processes described by D_i^0, $\bar{D}_i^0$ do not contribute to the overall be-

haviour significantly, we may also disregard D_i^0, $\bar{D}_i^0$. Thus evolution laws for $\boldsymbol{\sigma}^0$, θ^0, $\boldsymbol{\epsilon}_d^0$, $\boldsymbol{\epsilon}_s^0$ and $\mathbf{Z}^0$ are required and these will be discussed in the next chapter. Since $\dot{\boldsymbol{\epsilon}}_d^0$, $\dot{\boldsymbol{\epsilon}}_s^0$ do not cause changes of the internal energy, we finally have

$$\begin{aligned} S_i &= \{\boldsymbol{\sigma}^0, \theta^0, \mathbf{Z}^0\}, \\ \bar{S}_i &= \{\boldsymbol{\epsilon}_s^0, \boldsymbol{\epsilon}_d^0\}. \end{aligned} \tag{5.13}$$

5.2. Evolution laws

I. In the foregoing paragraph we have defined macromeasures of the instantaneous damage state. The complexity of the behaviour at the microscale prohibits the formulation and averaging of evolution laws for the microfields. Moreover, such a procedure is unnecessary as long as the misbs are considered "smeared out". Therefore we switch to a phenomenological description.

II. The evolution law for $\boldsymbol{\sigma}^0$ is proposed as

$$\dot{\boldsymbol{\sigma}}^0 = \mathbf{D}\dot{\boldsymbol{\sigma}} + \dot{\boldsymbol{\sigma}}^{0*}, \tag{5.14}$$

where, according to principle 3, the fourth-order tensor $\mathbf{D}$ and $\dot{\boldsymbol{\sigma}}^{0*}$ merely depend on $\boldsymbol{\sigma}$, θ, S_i, $\bar{S}_i$. The first term expresses that every change of macrostress amplifies the local stress concentrations. $\dot{\boldsymbol{\sigma}}^{0*}$ will describe the removal of stress concentrations due to local dislocation motion. At very high strain rates $\|\dot{\boldsymbol{\sigma}}^{0*}\| \ll \|\mathbf{D}\dot{\boldsymbol{\sigma}}\|$ and the stress concentration tensor increases till he eventually overcomes the threshold condition for damage initiation. The special choice

$$\mathbf{D}\dot{\boldsymbol{\sigma}} = d_1\dot{\boldsymbol{\sigma}} + d_2(\boldsymbol{\sigma}^0\dot{\boldsymbol{\sigma}} + \dot{\boldsymbol{\sigma}}\boldsymbol{\sigma}^0) + d_3(\mathbf{Z}^0\dot{\boldsymbol{\sigma}} + \dot{\boldsymbol{\sigma}}\mathbf{Z}^0) \tag{5.15}$$

will be applied in Sect. 9.

III. The evolution law for $\mathbf{Z}^0$ generally consists of three parts, namely

$$\dot{\mathbf{Z}}^0 = \dot{\mathbf{Z}}_n^0 + \dot{\mathbf{Z}}_g^0 + \dot{\mathbf{Z}}_c^0, \tag{5.16}$$

where n, g, c denote nucleation, growth and coalescence, respectively. In period 1 $\dot{\mathbf{Z}}_c^0$ may be neglected. We henceforth assume that the effects of nucleation and growth can be described by a single equation

$$\dot{\mathbf{Z}}^0 = \{d_z\}_z \langle\langle LC_z \rangle\rangle \mathbf{n}_z, \tag{5.17}$$

where $\{\ \}_z$ is associated to the yield condition

$$G_z := \boldsymbol{\sigma}^{0\prime} \cdot \boldsymbol{\sigma}^{0\prime} - \nu_z \operatorname{tr}\boldsymbol{\sigma}^0 - h_z \geqslant 0 \tag{5.18}$$

defined in $(\boldsymbol{\sigma}^0, \theta^0, S_i, \bar{S}_i)$-space and LC_z is given by

$$LC_z := \frac{\partial G_z}{\partial \boldsymbol{\sigma}^0} \cdot \dot{\boldsymbol{\sigma}}_{\text{inst}}^0 = (2\boldsymbol{\sigma}^{0\prime} - \nu_z \mathbf{1}) \cdot \mathbf{D}\dot{\boldsymbol{\sigma}}. \tag{5.19}$$

Equation (5.19) renders (5.17) rate-independent. This assumption is valid if $\dot{\mathbf{Z}}^0$ occurs either athermal (Frenkel's shear) or the relaxation time of thermally-activated mechanisms is sufficiently small.

The tensor $\mathbf{D}$ couples the loading condition for local processes with the rate of macrostress. Since damage continues during macroscopic unloading, $\mathbf{D}$ must not be positive

definite. In fact the functions d_i in Eq. (5.15) have to become negative for large $\mathbf{Z}^0$ (i.e., large strains).

From the definition (5.7) of $\mathbf{Z}^0$ it follows that $\mathbf{Z}^0$ is positive definite. A necessary condition to maintain the positive definiteness is

(5.20) $\dot{\mathbf{Z}}^0$ is positive definite.

We shall discuss the condition (5.20) in Sect. 8 along with the discussion of thermodynamics. $\mathbf{n}_z$, d_z will then be chosen in accord with this condition (5.20) and with the second law of thermodynamics.

IV. The flow rule for $\boldsymbol{\epsilon}_s^0 = \boldsymbol{\epsilon}_s$ is taken as follows:

$$\dot{\boldsymbol{\epsilon}}_s^0 = \{d_s\}_s \langle\langle\langle LC_s \rangle\rangle\rangle \mathbf{n}_s, \tag{5.21}$$

where $\{\ \}_s$ corresponds to the yield condition

$$G_s := \boldsymbol{\sigma}^{0\prime} \cdot \boldsymbol{\sigma}^{0\prime} - v_s \operatorname{tr} \boldsymbol{\sigma}^0 - h_s \geqslant 0 \tag{5.22}$$

and

$$LC_s = (2\boldsymbol{\sigma}^{0\prime} - v_s \mathbf{1}) \cdot \mathbf{D}\dot{\boldsymbol{\sigma}}. \tag{5.23}$$

V. The evolution laws for local dislocation motion and local temperature concentrations are taken to be

$$\dot{\boldsymbol{\epsilon}}_d^0 = \{\dot{\boldsymbol{\epsilon}}_d^{0*}\}_d, \quad \{\ \}_d \Leftrightarrow G_d := \boldsymbol{\sigma}^{0\prime} \cdot \boldsymbol{\sigma}^{0\prime} - h_d \geqslant 0, \tag{5.24}$$

$$\dot{\theta}^0 = \{d_{\theta s}\}_s \langle\langle\langle LC_s \rangle\rangle\rangle + \{d_{\theta d}\}_d. \tag{5.25}$$

6. Discussion of the macro-damage tensor, failure criteria

I. Two different failure criteria are required

a) a criterion for the nucleation of a macro-shear band and

b) a criterion for the assessment of damage due to misbs.

II. A useful indicator of shear band damage is the relative part ζ of shear band area of a reference plane $\Delta\mathbf{A} = \Delta A \mathbf{n}$

$$\zeta := \sum_{I_{\Delta A}} \frac{\delta A_\alpha}{\Delta A} |\mathbf{e}_\alpha \cdot \mathbf{n}|, \tag{6.1}$$

where the sum extends over all misbs cutting $\Delta\mathbf{A}$ (see Fig. 11). If ζ exceeds a threshold value ζ_{crit}, no further macro-shear stress can be transmitted. Therefore we postulate

$$\zeta < \zeta_{\text{crit}}. \tag{6.2}$$

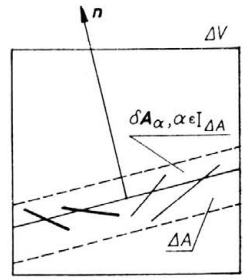

FIG. 11. Illustration of the damage measure ζ and the reference plane $\Delta\mathbf{A}$.

III. ζ itself is not a material property since it depends on $\mathbf{n}$. However, bounds of ζ can be expressed in terms of $\mathbf{Z}_m$ and finally in terms of $\mathbf{Z}^0$. Details can be found in [11]. We will present the main results:

$$\frac{\int\limits_{\Delta V_A} \mathbf{n}\cdot\mathbf{Z}_m\mathbf{n}dV}{\Delta V \Delta A} \leqslant \zeta \leqslant \frac{\sqrt{\int\limits_{\Delta V_A} ||\mathbf{Z}_m||^2 dV}}{\Delta A} N_{\text{misb}}, \tag{6.3}$$

where N_{misb} is the density of micro shear bands. The right inequality serves to render a more severe condition than the inequality (6.2)

$$N_{\text{misb}} \sqrt{\int\limits_{\Delta V_A} ||\mathbf{Z}_m||^2 dV} \leqslant \Delta A \zeta_{\text{crit}}. \tag{6.4}$$

We can prove

$$N_{\text{misb}} \leqslant K_1 ||\mathbf{Z}^0||^2, \qquad \sqrt{\int\limits_{\Delta V_A} ||\mathbf{Z}_m||^2 dV} \leqslant K_2 ||\mathbf{Z}^0|| \tag{6.5}$$

and thus arrive at the criterion

$$||\mathbf{Z}^0||^3 \leqslant K_3 \zeta_{\text{crit}} \tag{6.6}$$

in the case of a zeroth-order theory. However, a few rather crude estimates are involved in the derivation of the inequality (6.6) and one might ask for phenomenological generalizations. If there are no preferred shear band orientations, the inequality (6.6) may be restated by postulating that a strictly increasing isotropic function of $\mathbf{Z}^0$ must be bounded. In the case of two orthogonal preferred orientations (CFC-Test), the inequality (6.6) may be replaced by a strictly increasing orthotropic function of $\mathbf{Z}^0$. Nevertheless, the inequality (6.6) and its generalizations permit a judgement of damage due to micro-shear bands.

IV. As to the criterion for the nucleation of a macro-shear band, we propose:

Let $z_{\max}$ be the largest eigenvalue of $\mathbf{Z}^0$ and $\mathbf{e}_{\max}$ the corresponding eigenvector. Then a macro-shear band with area $||\mathbf{Z}^0||$ and normal $\mathbf{e}_{\max}$ is nucleated if $z_{\max}$ exceeds a threshold value z_{crit}.

To motivate this proposal, we assume that one of the shear bands (say $\delta\mathbf{A}_1$) is already large compared with the other $\delta\mathbf{A}_\alpha$, such that $\mathbf{Z}^0 \sim \delta\mathbf{A}_1 \mathbf{e}_1 \otimes \mathbf{e}_1$. However, $\mathbf{Z}^0\mathbf{e}_{\max} = z_{\max}\mathbf{e}_{\max}$ and thus $z_{\max} \sim \delta A_1$, $\mathbf{e}_{\max} = \mathbf{e}_1$.

7. Constitutive modelling of dislocation-induced deformation for strain rates between 10^{-5} s^{-1} and 10^4 s^{-1}

7.1. Internal and process variables, flow rules, evolution laws

I. Starting with the decomposition (4.3) of dislocation-induced strain, we will formulate general representations of flow rules and evolution laws. Throughout this paragraph we presuppose the existence of a variable u with the properties discussed ahead of Eq. (4.10). The present state of development of an appropriate evolution law for u will be studied in Sect. 7.2.

II. Neglecting the contribution of drag-controlled dislocation motion, we have

$$\dot{\boldsymbol{\epsilon}}_d = \dot{\boldsymbol{\epsilon}}_{da} + \dot{\boldsymbol{\epsilon}}_{dt}. \tag{7.1}$$

The flow rules for $\dot{\boldsymbol{\epsilon}}_{da}$, $\dot{\boldsymbol{\epsilon}}_{dt}$ will be chosen such that typical features of pure athermal or pure thermally-activated dislocation motion are rediscovered as special cases, i.e.

$\dot{\boldsymbol{\epsilon}}_{da}$ is described by a rate-independent flow rule and necessary conditions for $\dot{\boldsymbol{\epsilon}}_{da} \neq \mathbf{0}$ are the fulfillment of a yield condition and a loading condition;

$\dot{\boldsymbol{\epsilon}}_{dt}$ is described by a rate-dependent flow rule and is independent of a loading condition. Moreover, $\dot{\boldsymbol{\epsilon}}_{dt}$ depends on a yield condition such that $||\dot{\boldsymbol{\epsilon}}_{dt}||$ increases with positive values of the yield function.

To obtain familiar behaviour at small and moderate rates and small strains, a normality rule and symmetric behaviour under tension and compression is assumed for both parts of the dislocation-induced strain rate. We emphasize that $\dot{\boldsymbol{\epsilon}}_i = \dot{\boldsymbol{\epsilon}}_s^0 + \dot{\boldsymbol{\epsilon}}_{da} + \dot{\boldsymbol{\epsilon}}_{dt}$ is of course a non-associated and pressure-dependent flow rule due to the different secondary conditions of each part. Hardening and softening are described by internal variables D_i. For simplicity J_2-theories with isotropic and kinematic hardening are employed. We speculated about the subordinated significance of kinematic hardening at high strain rates in Sect. 2.3, but including kinematic hardening is an integral part of the ability to model behaviour of solids over a wide range of strain rates, particularly in connection with recovery effects after dynamic loading.

In the following we introduce an internal variable $\varkappa$, which is related to the total dislocation density N by

$$\varkappa = \varkappa_0 + \alpha N. \tag{7.2}$$

$\alpha \approx 5 \cdot 10^{-8}$ [Newton] is the constant introduced by ZSLODOS and KOVACS [54].

The relation (7.2) enables us to use the classical plastic work hypothesis of isotropic hardening with the "dislocation density" $\varkappa$ as an isotropic hardening parameter.

Now the following flow rules are introduced:

$$\dot{\boldsymbol{\epsilon}}_{da} = \{\gamma_a\}_a \langle LC_d \rangle \mathbf{n}_a, \tag{7.3}$$

where $\{\ \}_a$ relates to the yield condition

$$F_a := (\boldsymbol{\sigma}' - \mathbf{X}_a') \cdot (\boldsymbol{\sigma}' - \mathbf{X}_a') - g_a(\varkappa, u, \theta) \geqslant 0 \tag{7.4}$$

and LC_d is given by

$$LC_d := \frac{\partial F_a}{\partial \boldsymbol{\sigma}} \cdot \dot{\boldsymbol{\sigma}} + \frac{\partial F_a}{\partial \theta} \dot{\theta} = 2(\boldsymbol{\sigma}' - \mathbf{X}_a') \cdot \dot{\boldsymbol{\sigma}} - \frac{\partial g_a}{\partial \theta} \dot{\theta}. \tag{7.5}$$

$\mathbf{X}_a$ is the kinematic hardening tensor of athermal processes and the dependence of g_a on $u = N_m/N$ allows for the shift of the phenomenological yield stress σ_y with $\dot{\varepsilon}$. $\mathbf{n}_a$ may be taken as $\partial F_a/\partial \boldsymbol{\sigma}$. As to the thermally-activated processes, we suggest

$$\dot{\boldsymbol{\epsilon}}_{dt} = \{\dot{\boldsymbol{\epsilon}}_{dt}^*\}_t = \gamma_t \{\phi_t\}_t \mathbf{n}_t, \tag{7.6}$$

where the symbol $\{\ \}_t$ is associated to the yield condition

$$F_t := (\boldsymbol{\sigma}' - \mathbf{X}_t') \cdot (\boldsymbol{\sigma}' - \mathbf{X}_t') - g_t(\varkappa, u, \theta) \geqslant 0. \tag{7.7}$$

$\phi_t(F_t)$ with $\phi_t \to 0$ for $F_i \to 0$ is the usual overstress function. We emphasize that γ_t and ϕ_t are assumed to be bounded, i.e., no "control function" is required in contrast to the theory

of Perzyna and Pęcherski. The dominance of $\dot{\boldsymbol{\epsilon}}_{dt}$ at moderate total rates $\dot{\boldsymbol{\epsilon}}$ is described by an appropriate dependence of γ_a and γ_t on the "rate measure" u. The appearance of a small amount of $\dot{\boldsymbol{\epsilon}}_{da}$ at high rates is in contrast with Perzyna's theory; however, according to experiments and calculations by NOWACKI [35], the combined effect of $\dot{\boldsymbol{\epsilon}}_{da}$ and $\dot{\boldsymbol{\epsilon}}_{dt}$ gives better agreement with the data obtained from moderate velocity impact than the effect of $\dot{\boldsymbol{\epsilon}}_{dt}$ alone.

III. Internal and process variables

i. The quantity β with $\dot{\beta} = \alpha \dot{N}_m$, α taken from the relation (7.2) is a measure of mobile dislocation density in a polycrystal. β is decomposed into athermal and thermally-activated dislocations:

$$\beta = \beta_a + \beta_t. \tag{7.8}$$

Since the aforementioned experiments of SHIOIRI [47] were performed under conditions where thermal activation is assumed to dominate, we take

$$u = \frac{\beta_t}{\varkappa} \tag{7.9}$$

as the modified measure of strain rate. β_a, β_t are process variables.

ii. Our theory requires constitutive laws for $\mathbf{X}_a$, $\mathbf{X}_t$, $\varkappa$, β_a, β_t or $\mathbf{X}_a$, $\mathbf{X}_t$, $\varkappa$, β_a, u. For simplicity we assume that whenever there is a substantial contribution of β_a, that is for small $||\dot{\boldsymbol{\epsilon}}||$, we may use Gilman's approach (see [21]) of a state function:

$$\beta_a = \beta_a(\varkappa, \boldsymbol{\sigma}, \theta). \tag{7.10}$$

This assumption reduces the number of yet unknown evolution laws to four.

iii) We propose

$$\dot{\mathbf{X}}_a = \hat{c}_a \{\gamma_a\}_a \langle LC_d \rangle \mathbf{n}_{x_a} + \{\dot{\mathbf{X}}^*_{a,r}\}_a, \tag{7.11}$$

$$\dot{\mathbf{X}}_t = \{\dot{\mathbf{X}}^*_{t,g}\}_t + \{\dot{\mathbf{X}}^*_{t,r}\}_t, \tag{7.12}$$

$$\dot{\varkappa} = \boldsymbol{\sigma} \cdot (\dot{\boldsymbol{\epsilon}}_{da} + \dot{\boldsymbol{\epsilon}}_{dt}) - \dot{\varkappa}^*_r, \tag{7.13}$$

$$\dot{\beta}_t = \nu_{\beta d} \dot{\varkappa} - \dot{\beta}^*_t. \tag{7.14}$$

Here the first terms in Eqs. (7.11) and (7.12) describe the growth of the kinematic hardening tensors, which can be specialized to the well-known laws $\dot{\mathbf{X}}_{a,g} = c_a \dot{\boldsymbol{\epsilon}}_{da}$, $\dot{\mathbf{X}}_{t,g} = c_t \dot{\boldsymbol{\epsilon}}_{dt}$ by choosing $\mathbf{n}_{x_a} = \mathbf{n}_a$. $\dot{\mathbf{X}}^*_{a,r}$, $\dot{\mathbf{X}}^*_{t,r}$ and $\dot{\varkappa}^*_r$ are intended to describe recovery effects. The growth term $\nu_{\beta d} \dot{\varkappa}$ in Eq. (7.14) expresses that a certain fraction of new dislocations is nucleated immediately as thermally-activated mobile dislocations (cross slip). The task of $\dot{\beta}^*_t$ is to describe demobilization of mobile dislocations at weak obstacles and at high rates. Instead of Eq. (7.14), we will use the evolution law for u, resulting from Eqs. (7.13), (7.14). To focus attention on the basic problems, we neglect $\dot{\varkappa}^*_r$ in the following considerations. The equation for u thus reads:

$$\dot{u} = \varphi_1 \dot{\varkappa} - \varphi^*_2, \tag{7.15}$$

where

$$\varphi_1 = (\nu_d - u)/\varkappa, \quad \varphi^*_2 = \dot{\beta}^*_t/\varkappa. \tag{7.16}$$

Let us emphasize that u changes already in the elastic regime. Thus u may reach its value u_∞ corresponding to a given $\dot{\boldsymbol{\epsilon}}$ rapidly and min $(\sqrt{\frac{3}{2}\, g_a(u_\infty, \ldots)}, \sqrt{\frac{3}{2}\, g_t(u_\infty, \ldots)})$ is precisely the observed rate-dependent yield stress. The reason for the change of u in the range of macroscopically negligible inelastic deformations $\dot{\boldsymbol{\epsilon}}_d \approx \mathbf{0}$ may be found in the suppressing of local dislocation climb at high rates because vacancies are "frozen in". In the elastic range we introduce the notation

$$\dot{u} := \dot{u}_e = -\varphi_2^*. \tag{7.17}$$

7.2. The evolution of u

I. In this chapter we outline the requirements of an evolution law of u. We start with a discussion of uniaxial states of stress and isothermal processes. The mathematical requirements have been stated ahead of Eq. (4.10). From the physical point of view, u must be prescribed in terms of a functional of the history of external rates because every retardation (acceleration) of a process causes a remobilization (demobilization) of dislocations obstructed at weak obstacles (moving between weak obstacles). The expected behaviour of u in the elastic range is sketched in Fig. 12. The initial value $u = u_0$ remains unchanged for constant strain rate $k \approx 0$. With increasing k, u reduces to the value $u_\infty(k)$, shown in Fig. 12 by a dashed curve. The adaptation to the value u_∞ has to be finished for $\varepsilon < \varepsilon_y$ (yield strain), otherwise the yield stress would not fit with the given strain rate. Obviously u possesses a point of inflection. The trajectory of the projection of the inflection points onto the ε-k-plane is a curve $\varepsilon_{ip}(k)$, which for reasons of lucidity is not shown in Fig. 12.

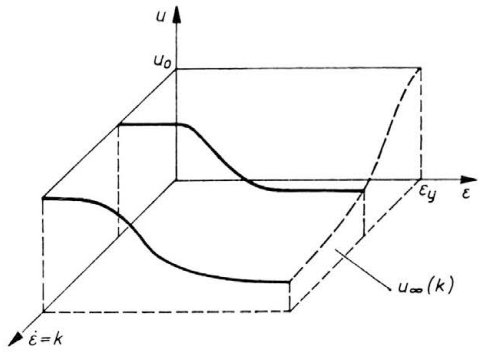

FIG. 12. Expected variation of u within the range of reversible deformations, k is a constant strain rate.

Different suggestions of an evolution law for u have been investigated in [11]. Unfortunately it turns out that simple first-order differential equations fail to describe the desired properties. A functional relation for $\ddot{u}_e$ is proposed as

$$\ddot{u}_e = -\Psi(\sigma)\left(\frac{\dot{\sigma}}{E\lambda}\right)^{n-1}\left[\frac{E}{\bar{\varepsilon}}\left\{\varepsilon_{ip}(\dot{\sigma}) - \frac{\sigma}{E}\right\}\frac{\dot{\sigma}}{E\lambda} - \int_0^\infty e^{-\lambda s}\dot{\sigma}_d^t(s)\,ds\right], \tag{7.18}$$

where Ψ, $\varepsilon_{ip}(\cdot)$ are material functions, n, λ, $\bar{\varepsilon}$ are material constants and E is Young's modulus; $\dot{\sigma}_d^t(s) := \dot{\sigma}(t-s) - \dot{\sigma}(t)$ is the difference history of stress rate. Though Eq. (7.18) appears to be fairly complicated, analytical solutions are possible in the case of constant

or piecewise constant stress rates $\dot{\sigma} = E\dot{\varepsilon} = Ek$. It can be shown that Eq. (7.18) fulfills the aforementioned requirements. Moreover, it neither contradicts principle 1 nor principle 2: In fact it may be shown by introducing the abbreviations $\xi_1 = \dot{u}$, $\xi_2 = \dot{\sigma}$ that the complete system of balance and constitutive laws is a quasi-linear hyperbolic system. Since u is a process variable, it does not influence the enthalpy and u or $\ddot{u}$ do not appear in the Clausius–Duhem-inequality. In the case of multiaxial states of stress, σ and $\dot{\sigma}$ are replaced by their second invariants. Further discussion can be found in [11].

II. The drawback of Eq. (7.18) becomes apparent in the range of inelastic behaviour where analytical solutions are impossible.

i. We start with a discussion of the question of existence of u_∞. Since we are dealing with a problem of dislocation mechanics, the answer should be independent of damage processes and we omit the damage variables from the very beginning of our considerations. For a given $\dot{\varepsilon} = \text{const}$, $\dot{\theta} = \text{const}$ the system of integrodifferential equations describing homogeneous processes comprises the equations for $\ddot{u} = (\varphi_1 \dot{\varkappa})^{\cdot} + \ddot{u}_e$, $\dot{\varkappa}$, $\dot{\varepsilon}_{da}$, $\dot{\varepsilon}_{dt}$, $\dot{x}_a$, $\dot{x}_t$ and $\dot{\sigma}$. These variables are arranged in a solution vector $\mathbf{w} = (u, \dot{u}, \varkappa, \varepsilon_{da}, \varepsilon_{dt}, x_a, x_t, \sigma)$ which is subjected to an equation of the type

$$\dot{\mathbf{w}} + \mathbf{a}(\mathbf{w}) + \int_0^\infty e^{-\lambda s} \mathbf{B}(s, \mathbf{w}) \mathbf{w}_d^t(s)\, ds = \mathbf{0}. \tag{7.19}$$

Now the possibility of solutions $\bar{\mathbf{w}} = (u_\infty, 0, \bar{\varkappa}, \bar{\varepsilon}_{da}, \bar{\varepsilon}_{dt}, \bar{x}_a, \bar{x}_t, \bar{\sigma}) = \bar{\mathbf{w}}(t)$ has to be examined. In the terminology of the stability theory this means that only two components of $\mathbf{w}$ are in equilibrium while the remaining components are time-dependent (The usual problem of the stability theory concerns the existence of equilibrium solutions $\mathbf{w} = \text{const}$). The existence of such a solution can be assured for linear systems with suitably chosen coefficients. In the case of nonlinear systems, sufficient conditions have been derived in [11], but they are far too complicated to give serviceable restrictions for the material functions.

At the present state of development we favour a kind of trial and error method with respect to the existence of u_∞. This means that physically meaningful material functions are chosen from other points of view and are tested numerically.

ii. We now look for the behaviour of Eq. (7.19) under perturbations of the constant strain and temperature rate. Due to the special choice of evolution laws, the derivative of Eq. (7.19) with respect to $\mathbf{w}$ exists and Eq. (7.19) may be linearized at $\bar{\mathbf{w}}$. Let $\mathbf{w}' = \bar{\mathbf{w}} + \delta\mathbf{w}$. Further assumptions on the hereditary integral lead to an equation

$$\delta\dot{\mathbf{w}} + \mathbf{A}\delta\mathbf{w} = \mathbf{R}, \tag{7.20}$$

where $\mathbf{A}$, $\mathbf{R}$ depend on $\bar{\mathbf{w}}(t)$ and explicitly on t. Compared with the literature on classical evolution laws, this again is an unusual problem [3]. If a fictitious equilibrium solution $\delta\bar{\mathbf{w}}$ is introduced as usual, Eq. (7.20) is replaced by

$$(\delta\mathbf{w} - \delta\bar{\mathbf{w}})^{\cdot} = \mathbf{A}(\delta\mathbf{w} - \delta\bar{\mathbf{w}}). \tag{7.21}$$

If $\mathbf{A}$ can be normalized (this places restrictions on the material functions) and is approximated by a constant matrix $\mathbf{A}_0$ in a sufficiently short time interval, a relaxation time of u can be derived from the eigenvalues of $\mathbf{A}_0$ (see [11]).

8. On continuum thermodynamics of high-strain-rate-deformations

I. The Clausius–Duhem inequality is assumed to be an appropriate characterization of irreversibility. We are searching for restrictions on the constitutive laws (5.14), (5.21), (5.25), (7.3), (7.6), (7.11)–(7.13) and the law determining the heat flux $\mathbf{q}$.

As to the heat flux, the simplest generalization of Fourier's law, which results in a hyperbolic equation of heat conduction, is Maxwell–Cattaneo's law:

$$\tau_q \dot{\mathbf{q}} + \mathbf{q} = -k \operatorname{grad} \theta, \tag{8.1}$$

where τ_q is the thermal relaxation time and k is the heat conductivity. Though the heat flux may often be neglected during high rate loading, $\mathbf{q}$ is substantial for the description of recovery in a body which is stressed and heated inhomogeneously after impact. As shown by KOSIŃSKI [23], Eq. (8.1) can be derived from the Clausius–Duhem inequality by supplementing the arguments of free enthalpy g with a vector-valued thermal variable $\boldsymbol{\alpha}_q$.

II. i. We define the free enthalpy g by

$$g = \frac{1}{\varrho} \boldsymbol{\sigma} \cdot \boldsymbol{\epsilon}_r - e + \eta\theta \tag{8.2}$$

(note that some authors use $-g$ instead of g), whereupon the Clausius–Duhem inequality reads

$$-\varrho \dot{g} - \varrho \eta \dot{\theta} - \boldsymbol{\epsilon}_r \cdot \dot{\boldsymbol{\sigma}} + \boldsymbol{\sigma} \cdot \dot{\boldsymbol{\epsilon}}_i - \frac{1}{\theta} \mathbf{q} \cdot \operatorname{grad} \theta \geqslant 0. \tag{8.3}$$

ii. In the present case

$$g = g(\boldsymbol{\sigma}, \theta; S_k, D_k, \boldsymbol{\alpha}_q) \tag{8.4}$$

and in view of principle 3 we employ

$$g = \mathscr{J}_e(\boldsymbol{\sigma}, \theta, \mathbf{Z}^0) + \mathscr{J}_s(\boldsymbol{\sigma}, \boldsymbol{\sigma}^0, \mathbf{Z}^0, \theta^0) + \mathscr{J}_d(\mathbf{X}_a, \mathbf{X}_t, \varkappa, \theta) + \mathscr{J}_q(\theta, \boldsymbol{\alpha}_q). \tag{8.5}$$

To rediscover Maxwell–Cattaneo's law, we use

$$\mathscr{J}_q = -\frac{1}{2} \frac{k}{\varrho \tau_q \theta} \boldsymbol{\alpha}_q \cdot \boldsymbol{\alpha}_q, \tag{8.6}$$

$$\dot{\boldsymbol{\alpha}}_q = \operatorname{grad} \theta - \frac{1}{\tau_q} \boldsymbol{\alpha}_q. \tag{8.7}$$

iii. Inserting the flow rules and evolution laws into the inequality (8.3) results in

$$\begin{aligned} &\left[\frac{\partial g}{\partial \boldsymbol{\sigma}} + \mathbf{D}^T \frac{\partial g}{\partial \boldsymbol{\sigma}^0} - \frac{1}{\varrho} \boldsymbol{\epsilon}_r + \langle\langle a_{s1} \rangle\rangle \mathbf{D}^T (2\boldsymbol{\sigma}^{0\prime} - \nu_z \mathbf{1}) + \langle\langle\langle a_{s2} \rangle\rangle\rangle \mathbf{D}^T (2\boldsymbol{\sigma}^{0\prime} - \nu_s \mathbf{1}) \right. \\ &\qquad \left. + 2 \{\gamma_a\}_a \langle a_{D1} \rangle (\boldsymbol{\sigma}' - \mathbf{X}_a') \right]_1 \cdot \dot{\boldsymbol{\sigma}} + \left[\frac{\partial g}{\partial \theta} - \eta - \{\gamma_a\}_a \langle a_{D1} \rangle \frac{\partial g_a}{\partial \theta} \right]_2 \dot{\theta} \\ &\qquad + \frac{\partial g}{\partial \boldsymbol{\sigma}^0} \cdot \dot{\boldsymbol{\sigma}}^{0*} + \frac{\partial g}{\partial \theta^0} \{d_{0d}\}_d + \frac{\partial g}{\partial \mathbf{X}_a} \cdot \{\dot{\mathbf{X}}_{a,r}^*\}_a + \frac{\partial g}{\partial \mathbf{X}_t} \cdot \{\dot{\mathbf{X}}_{t,g}^* + \dot{\mathbf{X}}_{t,r}^*\}_t \\ &\qquad + \left(\frac{1}{\varrho} + \frac{\partial g}{\partial \varkappa} \right) \boldsymbol{\sigma} \cdot \{\dot{\boldsymbol{\epsilon}}_{dt}^*\}_t - \frac{1}{\varrho \theta} \left(\frac{k}{\tau_q} \boldsymbol{\alpha}_q + \mathbf{q} \right) \cdot \operatorname{grad} \theta + \frac{k}{\varrho \tau_q^2 \theta} \boldsymbol{\alpha}_q \cdot \boldsymbol{\alpha}_q \geqslant 0. \end{aligned} \tag{8.8}$$

The abbreviations

$$a_{s1} = \{d_z\}_z(\partial g/\partial \mathbf{Z}^0)\cdot \mathbf{n}_z, \tag{8.9}$$

$$a_{s2} = \frac{\partial g}{\partial \theta^0}\{d_{\theta s}\}_s + (\boldsymbol{\sigma}\cdot \mathbf{n}_s)\{d_s\}_s, \tag{8.10}$$

$$a_{D1} = \hat{c}_a \frac{\partial g}{\partial \mathbf{X}_a}\cdot \mathbf{n}_{x_a} + \left(\frac{1}{\varrho} + \frac{\partial g}{\partial \varkappa}\right)(\boldsymbol{\sigma}\cdot \mathbf{n}_a) \tag{8.11}$$

have been used. The inequality (8.8) is linear in grad θ and we conclude that $\mathbf{q} = -(k/\tau_q)\boldsymbol{\alpha}_q$. With the help of Eq. (8.7) the law (8.1) is derived.

III. i. The objective of this paragraph is to introduce sufficient conditions for the validity of the inequality (8.8). First of all, we assume that the underlined term and the remaining expression on the left-hand side of the inequality (8.8) satisfy this inequality separately. Following LUBLINER [27], we secondly consider a high rate loading in the case of which

$$R := [\ ]_1\cdot \dot{\boldsymbol{\sigma}} + [\ ]_2\dot{\theta} \geqslant 0 \tag{8.12}$$

must hold since the remaining sum is independent of $\dot{\boldsymbol{\sigma}}$, $\dot{\theta}$ and can be made arbitrarily small by choosing large rates. Thus a sufficient condition for the inequality (8.12) is

$$\frac{1}{\varrho}\boldsymbol{\epsilon}_r = \frac{\partial g}{\partial \boldsymbol{\sigma}} + \mathbf{D}^T\frac{\partial g}{\partial \boldsymbol{\sigma}^0} + 2\lambda_d(\boldsymbol{\sigma}' - \mathbf{X}_a') + \lambda_{s1}\mathbf{D}^T(2\boldsymbol{\sigma}^{0\prime} - \nu_z\mathbf{1}) + \lambda_{s2}\mathbf{D}^T(2\boldsymbol{\sigma}^{0\prime} - \nu_s\mathbf{1}), \tag{8.13}$$

$$\eta = \frac{\partial g}{\partial \theta} - \lambda_d\frac{\partial g_a}{\partial \theta}, \tag{8.14}$$

and

$$0 \leqslant \lambda_d \leqslant \{\gamma_a\}_a a_{D1}, \quad 0 \leqslant \lambda_{s1} \leqslant a_{s1}, \quad 0 \leqslant \lambda_{s2} \leqslant a_{s2}. \tag{8.15}$$

The examination of unloading suggests $\lambda_d \equiv 0$, $\lambda_{s1} \equiv 0$, $\lambda_{s2} \equiv 0$ and from the inequalities (8.15) we find

$$\gamma_a a_{D1} \geqslant 0, \quad a_{s1} \geqslant 0, \quad a_{s2} \geqslant 0. \tag{8.16}$$

This is a first set of restrictions on the material functions. In place of Eqs. (8.13) and (8.14) we have

$$\boldsymbol{\epsilon}_r = \varrho\frac{\partial g}{\partial \boldsymbol{\sigma}} + \varrho\mathbf{D}^T\frac{\partial g}{\partial \boldsymbol{\sigma}^0}, \quad \eta = \frac{\partial g}{\partial \theta}. \tag{8.17}$$

ii. Concerning the remaining inequality, splitting in separate inequalities necessarily follows from the appearance of different secondary conditions. We arrive at

$$(\partial g/\partial \boldsymbol{\sigma}^0)\cdot \dot{\boldsymbol{\sigma}}^{0*} \geqslant 0, \tag{8.18}$$

$$(\partial g/\partial \theta^0)\{d_{\theta d}\}_d \geqslant 0, \tag{8.19}$$

$$(\partial g/\partial \mathbf{X}_a)\cdot \{\dot{\mathbf{X}}^*_{a,r}\}_a \geqslant 0, \tag{8.20}$$

$$\left(\frac{1}{\varrho} + \frac{\partial g}{\partial \varkappa}\right)\boldsymbol{\sigma}\cdot\{\dot{\boldsymbol{\epsilon}}^*_{dt}\}_t + \frac{\partial g}{\partial \mathbf{X}_t}\cdot\{\dot{\mathbf{X}}^*_{t,g} + \dot{\mathbf{X}}^*_{t,r}\}_t \geqslant 0. \tag{8.21}$$

The inequalities (8.16) and (8.18)–(8.21) comprise quite powerful restrictions to g and the other material functions. Though the validity of most inequalities can be guaranteed in

general (e.g., by choosing g as a sum of convex functions), it is more instructive to elaborate further consequences of the inequalities (8.16) and (8.18)–(8.21) in the light of the polynomial approximation of g presented in the next section.

IV. i. An approximation of the free enthalpy function: The state $\mathbf{Z}^0 = \mathbf{0}$, $\boldsymbol{\sigma}^0 = \mathbf{0}$, $\theta^0 = 0$, $\mathbf{X}_a = \mathbf{0}$, $\mathbf{X}_t = \mathbf{0}$, $\varkappa = 0$, $\boldsymbol{\alpha}_q = \mathbf{0}$ is a strong equilibrium state in CRISTESCU's terminology [8]. We will approximate g in the vicinity of this state by a polynomial P_g. It is assumed that P_g is an isotropic function of second degree in $\boldsymbol{\sigma}^0, \theta^0, \mathbf{X}_a, \mathbf{X}_t, \varkappa$ and of the third degree in $\boldsymbol{\sigma}, \theta$. The latter demand is due to CLIFTON [5]; third order terms are important in wave propagation studies. The $\mathbf{Z}^0$-dependence is chosen such that a) the requirement (5.20) is fulfilled and b) that the compliances increase with increasing damage according to the well-known effective stress concept in the continuum damage theory. Additional assumptions are involved about decoupling of $\mathbf{X}_a, \mathbf{X}_t$. Furthermore, let

$$\zeta^0 := ||\mathbf{Z}^0|| . \tag{8.22}$$

ii. Let P_g be given by

$$\begin{aligned} \varrho g = {} & \frac{1}{2}\lambda_{1/2}(\theta-\theta_0)^2 + \frac{1}{3}\lambda_{1/3}(\theta-\theta_0)^3 + \lambda_{2/1}(\theta-\theta_0)\operatorname{tr}\boldsymbol{\sigma} + \lambda_{2/2}(\theta-\theta_0)^2\operatorname{tr}\boldsymbol{\sigma} \\ & + \frac{\lambda_{3/0}}{2(1-k\zeta^0)}(\operatorname{tr}\boldsymbol{\sigma})^2 + \frac{\lambda_{3/1}(\theta-\theta_0)}{2(1-k\zeta^0)}(\operatorname{tr}\boldsymbol{\sigma})^2 + \frac{\lambda_{4/0}}{2(1-k\zeta^0)}\operatorname{tr}\boldsymbol{\sigma}^2 \\ & + \frac{\lambda_{4/1}(\theta-\theta_0)}{2(1-k\zeta^0)}\operatorname{tr}\boldsymbol{\sigma}^2 + \frac{\lambda_5}{3(1-k\zeta^0)}(\operatorname{tr}\boldsymbol{\sigma})^3 + \frac{\lambda_6}{1-k\zeta^0}(\operatorname{tr}\boldsymbol{\sigma})(\operatorname{tr}\boldsymbol{\sigma}^2) \\ & + \frac{\lambda_7}{3(1-k\zeta^0)}\operatorname{tr}\boldsymbol{\sigma}^3 - \frac{1}{2}\mu_1(\operatorname{tr}\boldsymbol{\sigma}^0)^2 - \frac{1}{2}\mu_2\operatorname{tr}\boldsymbol{\sigma}^{02} + \mu_3\operatorname{tr}(\boldsymbol{\sigma}'^2\mathbf{Z}^0) \\ & + \frac{1}{2}\mu_4\operatorname{tr}\mathbf{Z}^{02} + \frac{1}{2}\mu_5(\operatorname{tr}\mathbf{Z}^0)^2 + \frac{1}{2}\mu_6(\theta^0)^2 - \nu_1\boldsymbol{\sigma}\cdot\mathbf{X}_a - \nu_2\boldsymbol{\sigma}\cdot\mathbf{X}_t \\ & - \frac{1}{2}\nu_3\varkappa^2 + \nu_4\varkappa(\theta-\theta_0) - \frac{1}{2}\frac{k}{\tau_q\theta}\boldsymbol{\alpha}_q\cdot\boldsymbol{\alpha}_q \end{aligned} \tag{8.23}$$

with all $\nu_i \geqslant 0$, $\mu_i \geqslant 0$. For instance, an increase in $\varkappa$ causes hardening which means that the free energy increases and the free enthalpy as defined by the inequality (8.3) decreases, i.e., $\nu_3 \geqslant 0$. On the contrary, increasing damage causes softening and g increases, thus $\mu_4 \geqslant 0$, $\mu_5 \geqslant 0$. $\nu_4\varkappa$ is called "configurational entropy" and expresses the increase of η due to the production of lattice defects.

iii. From Eq. (8.23) one can easily calculate $\boldsymbol{\epsilon}_r$, η. The utilization of Eq. (8.23) in the context of the inequalities (8.16), (8.18)–(8.21) will be demonstrated in the case of the inequality (8.21). Assuming that growth of $\mathbf{X}_t$ is caused by $\dot{\boldsymbol{\epsilon}}_{dt}$, we choose $\dot{\mathbf{X}}^*_{t,g} = c_t(\cdot)\,\dot{\boldsymbol{\epsilon}}^*_{dt}$ and reform the inequality (8.21) as

$$\frac{1}{\varrho}[1 - \nu_3\varkappa + \nu_4(\theta-\theta_0) - \nu_2 c_t]\boldsymbol{\sigma}\cdot\dot{\boldsymbol{\epsilon}}_{dt} - \underline{\nu_2\boldsymbol{\sigma}\cdot\dot{\mathbf{X}}^*_{t,r}} \geqslant 0 . \tag{8.24}$$

The sign of the second term (underlined) can be found by the following consideration: $(\partial g/\partial \mathbf{X}_t)\cdot\dot{\mathbf{X}}^*_{t,g}$ must be negative in order to diminish the fraction of plastic work converted

into heat. This is correctly described by the $1-\nu_2 c_t$ instead of 1 in the bracketed term of the inequality (8.24). Thus,

$$(\partial g/\partial \mathbf{X}_t)\cdot \dot{\mathbf{X}}^*_{t,r} = -\nu_2 \boldsymbol{\sigma}\cdot \dot{\mathbf{X}}^*_{t,r} \geqslant 0 \tag{8.25}$$

has the opposite sign of the growth term and the second term fulfills the inequality (8.24) separately. As to the first term we require

$$1 > 1-\nu_3 \varkappa+\nu_4(\theta-\theta_0)-\nu_2 c_t > 0, \tag{8.26}$$

$$\boldsymbol{\sigma}\cdot \dot{\boldsymbol{\epsilon}}^*_{dt} \geqslant 0. \tag{8.27}$$

The magnitude of the expression (8.26) is estimated through measurements of stored energy and this magnitude can be achieved by choosing $\nu_3 = \hat{\nu}_3/\varkappa_{\max}$, $\hat{\nu}_3 \ll 1$ etc. Inequality (8.27) is fulfilled by deriving $\dot{\boldsymbol{\epsilon}}^*_{dt}$ from a convex potential, e.g., the one which is associated with the convex yield function (7.7). Therefore we may use

$$\{\dot{\boldsymbol{\epsilon}}^*_{dt}\}_t = \gamma_t \{\phi_t\}_t(\boldsymbol{\sigma}'-\mathbf{X}'_t), \quad \gamma_t > 0, \quad \phi_t \geqslant 0. \tag{8.28}$$

iv. Similar considerations can be applied in the case of the remaining evolution laws; we refer to [11]. The resulting equations are given below.

a) Damage variables

$$\dot{\mathbf{Z}}^0 = \frac{1}{\varrho}\{d_z\}_z l_z(\,\cdot\,)\left\{\mu_3 \boldsymbol{\sigma}'^2+\mu_4 \mathbf{Z}^0+\frac{k}{(1-k\zeta^0)^2\zeta^0}\Lambda(\boldsymbol{\sigma},\theta)\mathbf{Z}^0\right\}\langle\langle LC_z\rangle\rangle, \tag{8.29}$$

where Λ can be derived from g and d_z, $l_z \geqslant 0$ are functions to be determined independently of thermodynamic considerations.

$$\dot{\boldsymbol{\epsilon}}^0_s = \{l_s\}_s \langle\langle\langle LC_s\rangle\rangle\rangle \boldsymbol{\sigma}', \quad l_s \geqslant 0, \tag{8.30}$$

$$\dot{\boldsymbol{\sigma}}^0 = \mathbf{D}\dot{\boldsymbol{\sigma}}-l_{\sigma^0}\boldsymbol{\sigma}^{0\prime}-\bar{l}_{\sigma^0}(\operatorname{tr}\boldsymbol{\sigma}^0)\mathbf{1}, \quad l_{\sigma^0}, \bar{l}_{\sigma^0} \geqslant 0 \quad \text{vanish with } \boldsymbol{\epsilon}^0_d, \tag{8.31}$$

$$\dot{\theta}^0 = \{d_{0d}\}_d+\{d_{0s}\}_s\langle\langle\langle LC_s\rangle\rangle\rangle, \quad d_{0d} \geqslant 0, \quad d_{0s} \geqslant 0. \tag{8.32}$$

b) Dislocation variables

$$\dot{\boldsymbol{\epsilon}}_{da} = \{\gamma_a\}_a\langle LC_d\rangle(\boldsymbol{\sigma}'-\mathbf{X}'_a), \quad \gamma_a \geqslant 0, \tag{8.33}$$

$$\dot{\boldsymbol{\epsilon}}_{dt} = \gamma_t\{\phi_t\}_t(\boldsymbol{\sigma}'-\mathbf{X}'_t), \quad \gamma_t > 0, \quad \phi_t \geqslant 0, \tag{8.34}$$

$$\dot{\mathbf{X}}_a = c_a\dot{\boldsymbol{\epsilon}}_{da}-\{l_{x_a}\}_a(\boldsymbol{\sigma}'-\mathbf{X}'_a), \quad l_{x_a} \geqslant 0, \quad c_a > 0, \tag{8.35}$$

$$\dot{\mathbf{X}}_t = c_t\dot{\boldsymbol{\epsilon}}_{dt}-\{l_{x_t}\}_t(\boldsymbol{\sigma}'-\mathbf{X}'_t), \quad l_{x_t} \geqslant 0, \quad c_t > 0, \tag{8.36}$$

$$\dot{\varkappa} = \boldsymbol{\sigma}\cdot(\dot{\boldsymbol{\epsilon}}_{da}+\dot{\boldsymbol{\epsilon}}_{dt}). \tag{8.37}$$

Equations (8.29)–(8.37) are supplemented with the evolution laws for the process variables

$$\ddot{u} = (\nu_{\beta d}\dot{\varkappa})^{\cdot}-\Psi(\mathrm{II}^{\cdot}_{\sigma})\left(\frac{\mathrm{II}^{\cdot}_{\sigma}}{E\lambda}\right)^{n-1}\left[\frac{E}{\varepsilon}\left\{\varepsilon_{ip}(\mathrm{II}^{\cdot}_{\sigma})-\frac{\mathrm{II}_{\sigma}}{E}\right\}\frac{\mathrm{II}^{\cdot}_{\sigma}}{E\lambda}\right.$$
$$\left.-\int_0^{\infty} e^{-\lambda s}\mathrm{II}^{t}_{\dot{\sigma}d}(s)\,ds\right], \quad \mathrm{II}^{\cdot}_{\sigma} = \sqrt{\dot{\boldsymbol{\sigma}}\cdot\dot{\boldsymbol{\sigma}}}, \quad n > 2, \tag{8.38}$$

$$\dot{\boldsymbol{\epsilon}}^0_d = \gamma^0\{\phi^0\}_d\boldsymbol{\sigma}^{0\prime}; \tag{8.39}$$

the thermal and caloric equations of state, determining ϵ_r, η and derived from Eq. (8.23) according to Eqs. (8.17);

and the Mexwell–Cattaneo law (8.1).

Thus the set of constitutive laws is complete.

9. On some aspects of uniaxial wave propagation in a material with stress concentrators

I. We are interested in the influence of stress concentrations on wave propagation. It is well known from the theory of linear elastic composites that inclusions or fibrous particles have a pronounced influence on wave phenomena (dispersion, frequency dependent attenuation). However, sophisticated continuum theories are required for analytical investigations [1, 4], because the classical continuum theory and Hooke's law are unable to describe dispersion.

In this chapter, aspects of the propagation of uniaxial acceleration waves in undamaged solids with stress concentrators described by the stress concentration tensor $\boldsymbol{\sigma}^0$ will be investigated. On the wavefront and immediately behind the wavefront, the yield conditions are not satisfied and elastic overall behaviour prevails. Thus the results can be compared with an "effective modulus" approach in elasticity, which predicts the existence of simple waves and thus the wave profile remains unchanged. It will be interesting to see that according to our theory the wave profile changes during the propagation of the wavefront.

II. Uniaxial states of macrostress

i. Let x_1, x_2, x_3 be a Cartesian rectangular system of coordinates, x_1 being the direction of wave propagation. With respect to this system, the matrices of the different tensors are given by

$$\boldsymbol{\sigma} = \operatorname{diag}(\sigma, 0, 0), \quad \boldsymbol{\sigma}^0 = \operatorname{diag}(\sigma^0, \sigma_l^0, \sigma_l^0), \quad \boldsymbol{\epsilon} = \operatorname{diag}(\varepsilon, \varepsilon_l, \varepsilon_l),$$

where ε_l is lateral strain and σ_l^0 is the lateral component of $\boldsymbol{\sigma}^0$. For sufficiently small values of the initial value $\boldsymbol{\sigma}^0 = \boldsymbol{\sigma}_0^0$, the yield functions G_d, G_s, G_z are negative immediately behind the wavefront of the fastest wave and

$$\sigma, v, \theta, q, \sigma^0, \sigma_l^0, u \tag{9.1}$$

are the only time-dependent variables in this region. The particular evolution laws (5.15), (8.31) lead to $\dot{\sigma}_l^0 = 0$ for $\dot{\varepsilon}_d^0 = 0$ and σ_l^0 may be cancelled from the list (9.1).

ii. According to the above assumptions, the constitutive equations and balance laws describing uniaxial states of macrostress are as follows:

a) Evolution of reversible strain ($\dot{\varepsilon}_r = \dot{\varepsilon} = v'$, $(\,)'$: derivative with respect to x_1)

$$\dot{\sigma} - E_t v' + \hat{\alpha}_t \dot{\theta} + E_t m_{\sigma^0} \dot{\sigma}^0 = 0, \tag{9.2}$$

where E_t is the thermoelastic tangent modulus

$$E_t^{-1} = E^{-1} + (\lambda_{3/1} + \lambda_{4/1})(\theta - \theta_0) + 2(\lambda_5 + 3\lambda_6 + \lambda_7)\sigma,$$

$$\hat{\alpha}_t = [\alpha + 2\lambda_{2/2}(\theta - \theta_0) + (\lambda_{3/1} + \lambda_{4/1})\sigma]E_t =: \alpha_t E_t,$$

E — Young's modulus, α — coefficient of thermal expansion and m_{σ^0} is a function of ω^0 $\sigma_l^0 = \sigma_{l,0}^0$.

b) Law of heat flux

$$\dot{q}+\frac{k}{\tau_q}\theta' = -\frac{1}{\tau_q}q. \tag{9.3}$$

c) Evolution of u. If the material is at rest for $t < 0$, we find

$$\ddot{u} = -\Psi(\sigma)\left(\frac{\dot{\sigma}}{E\lambda}\right)^{n-1}\left[\frac{E}{\bar{\varepsilon}}\left\{\varepsilon_{ip}(\dot{\sigma})-\frac{\sigma}{E}\right\}\frac{\dot{\sigma}}{E\lambda}+\frac{\dot{\sigma}}{\lambda}(1-e^{-\lambda t})-\int_0^t e^{-\lambda s}\dot{\sigma}(t-s)\,ds\right]. \tag{9.4}$$

d) Evolution of σ^0

$$\dot{\sigma}^0 = \varphi\dot{\sigma}, \quad \varphi = \varphi(\sigma^0, \sigma_l^0). \tag{9.5}$$

e) Balance of momentum

$$\varrho\dot{v}-\sigma' = 0. \tag{9.6}$$

f) Balance of energy

$$\varrho c_\sigma\dot{\theta}-\theta\frac{\hat{\alpha}_t}{E_t}\dot{\sigma} = -q'+\frac{2}{\theta}q\left(\theta'+\frac{1}{k}q\right), \tag{9.7}$$

c_σ — specific heat at constant stress.

III. i. To render Eqs. (9.2)–(9.7) quasi-linear, it is necessary to introduce further variables according to

$$\dot{v} = \xi_1, \quad \dot{\sigma} = \xi_2, \quad \dot{\theta} = \xi_3, \quad \dot{q} = \xi_4, \quad \dot{u} = \xi_5, \quad \dot{\sigma}^0 = \xi_6 \tag{9.8}$$

and differentiate Eqs. (9.2), (9.3), (9.5)–(9.7) with respect to t. The final system of 12 equations can be arranged as

$$\mathbf{A}(\mathbf{w})\mathbf{w}_\tau+\mathbf{B}(\mathbf{w})\mathbf{w}_x+\mathbf{d}(\mathbf{w}) = \mathbf{0} \tag{9.9}$$

with

$$\mathbf{w} = (v, \sigma, \theta, q, u, \sigma^0, \xi_1, \xi_2, \xi_3, \xi_4, \xi_5, \xi_6) \tag{9.10}$$

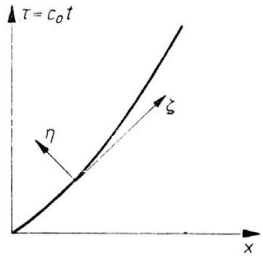

FIG. 13. Characteristic coordinates in the τ-x plane.

and $\tau = c_0 t$, $c_0 = \sqrt{E/\varrho}$ is introduced as a measure of time. The matrices **A**, **B** and the vector **d** are given in [11]. The inspection of the system (9.9) follows Clifton's method [3]: curvilinear orthogonal coordinates $\eta(x, \tau)$, $\zeta(x, \tau)$ (Fig. 13) are introduced such that $\eta = 0$ coincides with the wavefront and Eq. (9.9) reads

$$\mathbf{C}\mathbf{w}_\eta+\mathbf{T}\mathbf{w}_\zeta+\mathbf{d} = \mathbf{0}, \tag{9.11}$$

$$\mathbf{C} = \eta_\tau\mathbf{A}+\eta_x\mathbf{B}, \quad \mathbf{T} = \zeta_\tau\mathbf{A}+\zeta_x\mathbf{B}. \tag{9.12}$$

By definition all quantities with the exception of $\mathbf{w}_\eta$ are continuous across $\eta = 0$ and the jump $[\mathbf{w}_\eta]$ is proportional to the right eigenvector $\mathbf{r}$ of $\mathbf{C}$

$$[\mathbf{w}_\eta] = B(\zeta)\mathbf{r}. \tag{9.13}$$

The objective of this paragraph is the calculation of the variation of the jump amplitude $B(\zeta)$. One source of a variation of B is nonlinear thermoelastic behaviour through the third-order terms in the enthalpy function. To focus attention on the influence of stress concentrations, a restriction to linear thermoelastic behaviour ($\alpha_t = \alpha$, $E_t = E$) is employed in the subsequent calculations.

ii. The characteristic equation of the system (9.9) reads

$$0 = \det(c\mathbf{A}-\mathbf{B}) = (cc_0)^8\left[\varrho\tau_q\left\{\varrho c_\sigma(1+\varphi E m_{\sigma^0})+\frac{\alpha^2}{E}\theta\right\}(cc_0)^4\right. \tag{9.14}$$

$$\left.-\varrho\{c_\sigma E\tau_q+k(1+\varphi E m_{\sigma^0})\}(cc_0)^2+kE\right].$$

The existence of symmetric real-valued eigenvalues c can be read off from Eq. (9.14). The presence of stress concentrators has a presumably small quantitative influence on the wave speeds because $\varphi E m_{\sigma^0} \ll 1$ can be assumed. In the case of $\boldsymbol{\sigma}^0 = \mathbf{0}$, we have $m_{\sigma^0} = 0$ and the characteristic equation (9.14) may be transformed into the equation derived by KOSIŃSKI [23] if the relationship between the specific heats c_σ and c_ε is employed. The non-trivial wave speeds are

$$c_1 = \frac{1}{c_0}\sqrt{\omega_1+\omega_2} = -c_2, \qquad c_3 = \frac{1}{c_0}\sqrt{\omega_1-\omega_2} = -c_4,$$

$$\omega_1 = \frac{k+\tau_q c_\sigma E+\varphi E m_{\sigma^0} k}{2\tau_q\left[\varrho c_\sigma(1+\varphi E m_{\sigma^0})+\dfrac{\alpha^2}{E}\theta\right]}, \tag{9.15}$$

$$\omega_2 = \frac{\sqrt{\varrho^2[k(1+\varphi E m_{\sigma^0})+\tau_q c_\sigma E]^2-4\varrho\tau_q kE\left[\varrho c_\sigma(1+\varphi E m_{\sigma^0})+\dfrac{\alpha^2}{E}\theta\right]}}{2\tau_q\left[\varrho c_\sigma(1+\varphi E m_{\sigma^0})+\dfrac{\alpha^2}{E}\theta\right]}.$$

We confine ourselves to the study of fast waves propagating in positive x_1-direction, i.e., $c = c_1(\theta, \sigma^0, \sigma_l^0)$. The transport equation for B reads

$$(l_a T_{ab} r_b)\frac{dB}{d\zeta}+\left\{l_a\frac{\partial T_{ab}}{\partial w_c}\frac{\partial w_b}{\partial\zeta}r_c+l_a\frac{\partial d_a}{\partial w_b}r_b+l_a T_{ab}\frac{\partial r_b}{\partial\zeta}\right\}B+ \tag{9.16}$$

$$+\left(l_a\frac{\partial C_{ab}}{\partial w_c}r_b r_c\right)B^2 = 0, \qquad a,b,c = 1,\ldots,12,$$

where the summation convention is applied. $\mathbf{l}$, $\mathbf{r}$ are left and right eigen-vectors of $\mathbf{C}$, whose calculation has been omitted here for the sake of brevity.

For propagation into a macroscopically homogeneous medium and in the case of the employed constitutive laws, the underlined terms in Eq. (9.16) vanish. Consequently,

$$(\mathbf{l}\cdot\mathbf{Tr})\frac{dB}{d\zeta}+\left(\mathbf{l}\cdot\frac{\partial\mathbf{d}}{\partial\mathbf{w}}\mathbf{r}\right)B=0,$$
$$\mathbf{l}\cdot\mathbf{Tr}=4\varrho c_0+\Delta,\qquad |\Delta(\boldsymbol{\sigma}^0,\theta)|\ll 4\varrho c_0. \tag{9.17}$$

The coefficient $\mathbf{l}\cdot(\partial\mathbf{d}/\partial\mathbf{w})\mathbf{r}\neq 0$ is a quite complicated function of θ, $\boldsymbol{\sigma}^0$. Thus the stress concentration tensor influences the wave profile in a highly nonlinear way. The orientation of stress concentrators like elongated particles makes itself conspicuous via the dependence on σ^0, σ_l^0.

10. Summary and conclusions

In this paper we have presented the general frame of a constitutive model of inelastic behaviour as a consequence of the combined effects of dislocation motion and shear band processes. We claim the validity of this model for a wide range of strain rates up to $10^4\ s^{-1}$ and for predominantly radial loading histories like vertical impact with subsequent recovery. The latter restriction follows from the simplified modelling of dislocation processes and the accompanying hardening effects through single yield surfaces and associated flow rules for $\dot{\boldsymbol{\epsilon}}_{da}$, $\dot{\boldsymbol{\epsilon}}_{dt}$.

In comparison with related papers we emphasize the following aspects of our model:

a) the use of internal variables characterizing local disturbances and the application of these variables in yield functions;

b) the approximate method of homogenization, leading to the series expansions (5.6). This method seems to be very promising in connection with other damage effects like composite damage and deserves further investigation;

c) the utilization of a measure u of strain rate and temperature rate;

d) the consideration of thermodynamics.

Future work will be directed towards:

a) the determination of material functions and application to problems with radial loading and strain rates less than $10^4\ s^{-1}$;

b) the extension of the theory with special regard paid to: 1) the description of the behaviour in period 2, i.e., after the nucleation of a macrodefect, 2) the incorporation of viscous drag-controlled dislocation motion, 3) the incorporation of other damage mechanisms.

Acknowledgement

The research of the authors that is described here has been supported by the Frannhofer-Gesellschaft. This support is greatfully acknowledged.

References

1. J. D. ACHENBACH, *A theory of elasticity with microstructure for directionally reinforced composites*, CISM Courses and Lectures, 167.
2. R. J. ASARO, *Micromechanics of crystals and polycrystals*, Adv. Appl. Mech., **23**, 2–117, 1983.

3. E. BECKER, *Gasdynamik*, BG Teubner, Stuttgart 1969.
4. A. BEDFORD, D. S. DRUMHELLER and H. J. SUTHERLAND, *On modelling the dynamics of composite materials*, Mechanics Today, 3, 1978.
5. R. J. CLIFTON, *Plastic waves, theory and experiment*, Mechanics Today, 1, 1972.
6. R. J. CLIFTON and P. KUMAR, *Dislocation configurations due to plate impact*, in [20].
7. R. J. CLIFTON, *Experiments and micromechanics of viscoplasticity*, in: G. BIANCHI and A. SAWCZUK [Eds.], Plasticity Today, Elsevier, 1985.
8. N. CRISTESCU and I. SULICIU, *Viscoplasticity*, M. Nijhoff Publ., 1982.
9. D. R. CURRAN, *Dynamic fracture*, in: J. A. ZUKAS, T. NICHOLAS, H. F. SWIFT, L. B. GRESCZUK, D. R. CURRAN [Eds.], Impact Dynamics, J. Wiley and Sons, 1982.
10. D. R. CURRAN, L. SEAMAN and D. A. SHOCKEY, *Linking dynamic fracture to microstructural processes*, in [31].
11. H. DIEHL, W. FORNEFELD and O. T. BRUHNS, *Material behaviour under dynamic loading*, Report 1987 for the Fraunhofer-Gesellschaft [in German].
12. P. S. FOLLANSBEE, *High strain rate deformation of FCC metals and alloys*, in [34].
13. H. J. FROST and M. F. ASHBY, *Deformation-mechanics maps*, Pergamon Press, 1982.
14. J. J. GILMAN, *The microdynamics of plastic flow*, in [44].
15. J. HARDING [Ed.], *Mechanical properties at high rates of strain*, The Institute of Physics, 1974.
16. J. HARDING [Ed.], *Mechanical properties at high rates of strain*, The Institute of Physics, 1984.
17. J. D. JACKSON, *Classical electrodynamics*, J. Wiley and Sons, 1975.
18. S. KALISZKY, *Dynamic plastic response of structures*, in: G. BIANCHI and A. SAWCZUK [Eds.], Plasticity Today, Elsevier, 1985.
19. TH. V. KÁRMÁN and P. DUWEZ, *The propagation of plastic deformation in solids*, J. Mech., **21**, 987–994, 1950.
20. K. KAWATA and J. SHIOIRI [Eds.], *High velocity deformation of solids*, IUTAM Symposium, Tokyo 1977, Springer, 1978.
21. J. M. KELLY, *Dislocation models in continuum laws*, in: K. C. VALANIS [Ed.], Constitutive Models in Viscoplasticity-Phenomenological and Physical Aspects, ASME, AMD, **21**, 1976.
22. J. R. KLEPACZKO, *On advanced constitutive modelling of rate sensitivity. Temperature and strain hardening in FCC and BCC metals*, in: C. Y. CHIEM, H. D. KUNZE, L. W. MEYER [Eds.], *Impact loading and dynamic behaviour of materials*, DGM, 1988.
23. W. KOSIŃSKI, *Thermal waves in inelastic bodies*, Arch. Mech., **27**, 733–748, 1975.
24. A. KRAWIETZ, *Materialtheorie*, Springer-Verlag, 1986.
25. E. KRÖNER and C. TEODOSIU, *Lattice defect approach to plasticity and viscoplasticity*, in [44].
26. A. KUMAR and R. G. KUMBLE, *Viscous drag on disclinations at high strain rates in copper*, J. Appl. Physics, **40**, 3475–3480, 1969.
27. J. LUBLINER, *On the structure of the rate equations of materials with internal variables*, Acta Mech., **17**, 109–119, 1973.
28. L. E. MALVERN, *Experimental and theoretical approaches to characterization of material behaviour at high rates of deformation*, in [16].
29. J. B. MARTIN and P. S. SYMONDS, *Mode approximations for impulsively-loaded rigid-plastic structures*, J. Engng. Mech. Div. Proc. ASCE, **92**, 5, 43–66, 1966.
30. H. MECKING and K. LÜCKE, *A new aspect of the theory of flow stress of metals*, Scripta Metall., 4, 427–432, 1970.
31. M. A. MEYERS and L. E. MURR [Eds.], *Shock waves and high-strain-rate phenomena in metals*, Plenum Press, 1981.
32. M. A. MEYERS and L. E. MURR, *Defect generation in shock-wave deformation*, in [31].
33. T. MURA, *Micromechanics of defects in solids*, M. Nijhoff Publ., 1982.
34. L. E. MURR, L. P. STAUDHAMMER and M. A. MEYERS, *Metallurgical applications of shock-wave and high-strain-rate phenomena*, M. Dekker Inc., 1986.
35. W. K. NOWACKI, *Thermal effects in dynamic plasticity. Numerical solution and experimental investigations*, in [41].

36. P. PERZYNA, *Fundamental problems in viscoplasticity*, Adv. Appl. Mech., **9**, 243–377, 1966.
37. P. PERZYNA, *Internal variable description of plasticity*, in [44].
38. P. PERZYNA, *The constitutive equations describing thermomechanical behaviour of materials at high rates of strain*, in [15].
39. P. PERZYNA and R. B. PĘCHERSKI, *Modified theory of viscoplasticity. Physical foundations and identifications of material functions for advanced strains*, Arch. Mech., **35**, 423–436, 1983.
40. P. PERZYNA, *Constitutive modelling for brittle dynamic fracture in dissipative solids*, Arch. Mech., **38**, 725–738, 1986.
41. J. PHILIBERT [Ed.], Proc. Conference on Mechanical and Physical Behaviour of Materials under Dynamic Loading DYMAT 85, J. de Physique, C-5, 1985.
42. T. PINTAT, L. W. MEYER and H. SCHRADER, *Properties of inhomogeneous shear zones in different materials*, in [41].
43. R. RAJ and M. F. ASHBY, *Intergranular fracture at elevated temperature*, Acta Metall., **23**, 653–666, 1975.
44. A. SAWCZUK [Ed.], *Problems of plasticity*, Noordhoff Int. Publ., 1974.
45. L. SEAMAN, D. R. CURRAN, D. C. ERLICH, T. COOPER, O. DULLUM, *Shear band observations and derivations of requirements for a shear band model*, in [41].
46. J. SHIOIRI, K. SATOH and K. NISHIMURA, *Experimental studies on the behaviour of dislocations in copper at high rates of strain*, in [20].
47. J. SHIOIRI and K. SATOH, *An ultrasonic study of the rate controlling mechanism of dislocation motion at high rates of strain*, in [41].
48. D. A. SHOCKEY, D. R. CURRAN and L. SEAMAN, *Computer modelling of microscopic failure processes under dynamic loads*, in [20].
49. D. A. SHOCKEY and D. C. ERLICH, *Metallurgical influences on shear band activity*, in [31].
50. D. A. SHOCKEY, *Materials aspects of the adiabatic shear phenomenon*, in [34].
51. R. B. STOUT, *Analysis of dislocation kinetics across shocks*, in [34].
52. P. S. SYMONDS and C. T. CHON, *Approximation techniques for impulsive loading of structures of time dependent plastic behaviour with finite deflections*, in [15].
53. G. I. TAYLOR, *The use of flat-ended projectiles for determining dynamic yield stress. Part I*, Proc. Roy. Soc. London, A 194, 289–299, 1948.
54. I. ZSLODOS and I. KOVACS, *Dislocations and plastic deformation*, Oxford 1973.

INSTITUT FÜR MECHANIK
RUHR-UNIVERSITÄT BOCHUM, FRG.

Received November 2, 1987.